Authors' response for "Impact of atomic chlorine on the modelling of methane and its $^{13}CH_4$:$^{12}CH_4$ isotope ratio at global scale"

Joël Thanwerdas[1,*], Marielle Saunois[1], Antoine Berchet[1], Isabelle Pison[1], Didier Hauglustaine[1], Michel Ramonet[1], Cyril Crevoisier[2], Bianca Baier[3,4], Colm Sweeney[4], and Philippe Bousquet[1]

[1]Laboratoire des Sciences du Climat et de l'Environnement, CEA-CNRS-UVSQ, IPSL, Gif-sur-Yvette, France.
[2]Laboratoire de Météorologie Dynamique, École Polytechnique, IPSL, Palaiseau, France.
[3]Cooperative Institute for Research in Environmental Sciences (CIRES), University of Colorado-Boulder, Boulder, CO, USA 80305
[4]NOAA Earth System Research Laboratory Global Monitoring Division, Boulder, CO, USA 80305

Correspondence: J. Thanwerdas (joel.thanwerdas@lsce.ipsl.fr)

1 Introduction

We thank the referees for their time and for giving fruitful comments and reviews to our manuscript. It helped improving our manuscript substantially. We address below their comments and our corresponding corrections to the manuscript. Comments from Referees #1 and #2 are reported below in blue and red respectively. We include point-by-point replies and corresponding corrections to the manuscript are included in bold between horizontal lines. The marked-up manuscript is added at the end of this response.

2 General comments

It is necessary to let a native English speaker edit and improve the entire manuscript; in the current state, it is difficult to read (excessive use of definite articles, clumsy sentence composition, etc.).

We thoroughly proof-read the manuscript and made a lot of corrections in order to provide an English writing as good as possible. The manuscript has also been proof-read by two native English speakers.

I am concerned about the adequacy of the model setup, namely the adopted INCA fields: are these obtained using consistent atmospheric dynamics (i.e. driven from similar nudging data)? If not, oxidants fields may quite not correspond the offline model.

The INCA fields used in our study are indeed obtained using consistent atmospheric dynamics as INCA chemistry scheme was coupled to the LMDz online version, which provided the mass-fluxes prescribed in the LMDz offline version. Details have been added to the Section 2.3 (P5 L7-10) in order to make it clearer for readers :

The three-dimensional and time-dependent oxidant concentration fields (OH, O(^{1}D) and Cl) were simulated by the

LMDz GCM (described in Section 2.1) coupled to the chemistry scheme INCA [INteraction with Chemistry and Aerosols] (Folberth et al., 2006; Hauglustaine et al., 2004). The mass fluxes used in the offline version of LMDz were calculated by the online version of LMDz nudged to the same meteorological data.

If there is an explicit representation of CH_4 isotopologues in the model, why do you use "negative emission" apparatus and Eq.(5) instead of explicitly simulating soil uptake via isotopologues with respective fractionation in the surface layer? I cannot confirm the correctness of the approach used here, because I do not see what for δ^{13}Ceff is introduced. From Eq.(5) it follows that δ^{13}Ceff is the isotope composition of the uptake flux, depleted in 13C w.r.t. to the surface layer burden. The latter becomes enriched in 13C upon uptake, in proportion to the removal flux. The dynamic equilibration of these processes results in δ^{13}Camb, however you cannot take the latter in Eq.(5) because you will introduce additional fractionation. In other words, the uptake flux should be calculated from 13C/12C simulated in the model, not the "ambient" signature. If you are certain this is an admissible approach, please quantify the error introduced it.

Could you explain this equation further? Simply substituting numbers does not seem to provide δ^{13}Ceff to be – 65.9 ‰ (1 – 47.2)/1.02 – 1= – 46.3, and following equations presented in Snover and Quay (2000), δ^{13}Csoil = δ^{13}Catm + (1/KIE soil -1)*1000, it will lead to δ^{13}Csoil = – 66.8 ‰ (assuming δ^{13}Catm = – 47.2 ‰ and KIE soil =1.02).

We apologize for not explaining equation (5) further in the submitted version. The result from Snover and Quay (2000) seems to be only a simplification of our equation (5) considering that KIE_{soil} value is really close to 1. Please, note that in order to use our formula, δ^{13}C-CH_4 values must not be used in permil, i.e. rather use -47.2/1000 = -0.0472 and not -47.2. The full demonstration is provided below, although we do not use this method (and this equation) in the revised version as explained hereafter. We recognize that using a prescribed soil sink flux as done so far in our model, does not fully consider changes in ambient isotope methane and introduced simplification (and maybe small errors). Also, referee #2 pointed out that prescribing a constant value to the soil sink isotopic signature using a formula that relies on the atmospheric δ^{13}C-CH_4 signal could result in an error. We have then addressed this issue by changing our method. We now implement the soil sink into the model and prescribe a KIE value (see Text S2 in the supporting information or just below). Due to LMDz specificities, this method was not easy to implement and we did not do that in the first place because we assumed that final δ^{13}C-CH_4 values at the surface would not be largely modified and more importantly the differences between them would not be affected. In the revised manuscript, the new method is applied. It turned out that the final δ^{13}C-CH_4 from Figure 8 are slightly modified (between 0.03 ‰ and 0.06 ‰ depending on the scenario), hence also slightly changing the differences. A few numbers have been modified in the manuscript, although not affecting the conclusions.

Demonstration of Equation 5 of the submitted manuscript:

Let L_{12} and L_{13} be the chemical losses of $^{12}CH_4$ and $^{13}CH_4$ through the soil sink, respectively. k_{12} and k_{13} are the associated reaction constants. M_{12}, M_{13} and M_{air} are the molar masses of $^{12}CH_4$, $^{13}CH_4$ and dry air, respectively. $[^{12}CH_4]$ and $[^{13}CH_4]$

are the ambient concentrations of $^{12}CH_4$ and $^{13}CH_4$ at the surface. $\delta^{13}C_{amb}$ is the associated isotopic signal. KIE_{soil} is defined such that :

$$KIE_{soil} = \frac{k_{12}}{k_{13}} \tag{1}$$

We also have, by definition :

$$L_{12} = k_{12} \times [^{12}CH_4] \tag{2}$$

$$L_{13} = k_{13} \times [^{13}CH_4] \tag{3}$$

$$[^{13}CH_4] = (1 + \delta^{13}C_{amb}) \times R_{V-PDB} \times [^{12}CH_4] \tag{4}$$

We define $\delta^{13}C_{eff}$ the soil sink effective isotopic signature :

$$\delta^{13}C_{eff} = \frac{\frac{L_{13}}{L_{12}}}{R_{V-PDB}} - 1 \tag{5}$$

By dividing (3) and (2) and using (4), we can get :

$$\frac{L_{13}}{L_{12}} = \frac{[^{13}CH_4]}{[^{12}CH_4]} \times \frac{1}{KIE_{soil}} \tag{6}$$

$$\Rightarrow \delta^{13}C_{eff} = \frac{[^{13}CH_4]}{[^{12}CH_4]} \times \frac{1}{R_{V-PDB}} \times \frac{1}{KIE_{soil}} - 1 \tag{7}$$

$$\Rightarrow \delta^{13}C_{eff} = \frac{1 + \delta^{13}C_{amb}}{KIE_{soil}} - 1 \tag{8}$$

Text S2:

Here we describe the methods use to infer a pseudo-chemical soil sink from the initial negative-flux grid map. We therefore define here a soil pseudo-chemical field (SPCF) and a soil pseudo-species (we call it X). In others terms, we replace the Equation (1) below (that represents the methane removal by the soil sink) by the Equation (2) also below :

$$\frac{d[CH_4]_1}{dt} = \frac{S_{\text{soil}} \times A}{m_{\text{air}}} \frac{M_{\text{air}}}{M_{\text{CH}_4}} \tag{9}$$

$$\frac{d[CH_4]_2}{dt} = -k \times [CH_4]_2 \times [X] \tag{10}$$

S_{soil} is here the initial negative-flux soil sink in $\text{kg m}^{-2}\,\text{s}^{-1}$. A is the surface area. m_{air}, M_{air} and M_{CH_4} are the molar masses of dry air and CH_4, respectively. $[CH_4]$ is CH_4 mixing ratios in mol mol^{-1} and $[X]$ is X concentrations in molecules cm^{-3}. k is the reaction constant in $\text{cm}^3\ \text{molecules}^{-1}\,\text{s}^{-1}$. For simplicity reason, we set k equal to 1 $\text{cm}^3\ \text{molecules}^{-1}\,\text{s}^{-1}$.

This method allows to implement a soil sink in LMDz as it is done with the other chemical species (OH, $O(^1D)$, and Cl) and prescribe a KIE_{soil}. The reaction between CH_4 and X resulting from this method must lead to the same CH_4 removal as with the initial grid map, i.e. having :

$$\frac{d[CH_4]_1}{dt} = \frac{d[CH_4]_2}{dt} \tag{11}$$

As the soil sink is only active at the surface, the SPCF is equal to zero at all levels except at the surface. The equation giving the pseudo-species mixing ratios in mol mol^{-1} at the surface is :

$$[X] = \frac{S_{soil} \times A}{m_{air}} \frac{M_{air}}{M_{CH_4}} \times \frac{1}{[CH_4]} \tag{12}$$

$[CH_4]$ is the CH_4 mixing ratio in mol mol^{-1}.

X concentrations in equation (2) are inferred considering that the soil sink intensity must be strictly equal in both methods, therefore CH_4 mixing ratios are not modified. As $[X]$ is dependent on $[CH_4]$, we run a first simulation to retrieve CH_4 mixing ratios at the surface with the initial negative-flux soil sink.

Arriving at a proper dynamically equilibrated isotope CH_4 distribution up to mesosphere for a given year of the present is a difficult task (also because of not equilibrated CH_4 burden). History of CH_4 transport is still present in the UTLS (where CH_4 lifetime can reach 100 years) up to middle stratosphere, so taking just year 2000 emissions is not a satisfactory approach (as compared to, e.g., at least taking 1980- 2000 CH_4 emissions). A least uncertain way here is to prescribe transient mixing and isotope ratios at the surface and let the model run for 1980-2000 to "populate" atmosphere with CH_4 isotopologues, in hope that transport and atmospheric sinks are adequate. To recap: to ascertain the results of simulations starting from such obtained initial conditions, you need to show in this work that your spin-up method is adequate, i.e. by estimating errors or comparing to other simulations using pre-2000 CH_4 emissions and atmospheric distribution.

We agree that having a good isotope CH_4 distribution up to the mesosphere for a given year is difficult. We did not process emissions from 1980 to 2000 and the work to infer them is expected to be overwhelming. We already initialized the spin-up using realistic initial conditions (as explained in the manuscript) so populating should take much less time than starting from an "empty" atmosphere. Also, using prescribed transient mixing and isotope ratios at the surface do not appear to us as a good solution as it implies to regulate total methane mass too. As the mass in the stratosphere, region of interest, exhibit a high uncertainty, we think that using this method would increase even more the uncertainties. In order to address the comment, we increased the spin-up time to 30 years instead of 19 years. It is true that methane needed a larger time to reach stability at all levels. The methane isotope ratio between 20km and 70km reaches stability quickly (less than 5 years). Below this altitude, increasing the spin-up time slightly changed global values. At the surface, it shifted the initial conditions (global mean) in 2000 from -47.2 ‰ to -47.15 ‰. Moreover, our study aims to compare scenarios with varying chlorine between them and to assess the impact of the Cl sink. Uncertainties on source isotopic signatures and categories share in the global budget are high enough

not to expect a perfect match between observed and simulated isotope ratio. Modifications in Section 2.7 (P9 L14 - P10 L10) are below :

We perform one reference simulation (REF) and a set of 7 sensitivity tests (Table 5) with different Cl concentrations in the troposphere and in the stratosphere. We simulate in parallel $^{12}CH_4$ and $^{13}CH_4$ mixing ratios for the 2000-2018 period starting from the same initial conditions, and using monthly varying CH_4 emissions (see Sect. 2.5). CH_4 is defined as the sum of the two tracers.

The initial conditions for the REF simulation have been obtained using a 30-year spin-up using emissions and meteorology for the year 2000 including all chemical sinks in order to obtain a good spatial and vertical distribution of CH_4 mixing ratios and δ^{13}C-CH_4 values. For the spin-up run, CH_4 mixing ratios from Locatelli et al. (2015) inferred using an inversion system were used as initial conditions for total CH_4. Additionally, δ^{13}C-CH_4 values inferred from globally averaged observations were prescribed at the surface and the Rayleigh fractionation equation was applied to infer a realistic δ^{13}C-CH_4 vertical profile.

There is a 0.04 ‰ difference between the observed δ^{13}C-CH_4 global mean at the surface (based on available NOAA-GGGRN δ^{13}C-CH_4 surface observations) in 2000 and the output from the spin-up. No adjustment is performed due to non-linearity of transport, mixing and fractionating sink processes. From these initial conditions, we run an ensemble of scenarios spanning 2000-2018 using transient emissions, and varying the Cl sink of CH_4. Sensitivity test characteristics are summarized in Table 5.

A more concerning issue is the subsequent “adjustment of the simulated isotopic signal” to “obtain satisfying initial conditions”. How is this adjustment performed and on which grounds? I am not aware of a method that allows adjusting 3D fields of $^{12}CH_4$ and $^{13}CH_4$ to some surface observations. The non-linearity of transport, mixing and fractionating sink processes does not allow this. Furthermore, if such adjustment is required, it implies your initial conditions for the experiments are erroneous. Until this issue is clarified, I see no point considering the results of the simulations.

We fully understand this concern and decided to remove this adjustment. As Referee #2 indicated it, the non-linearity of transport, mixing and fractionation may not allow this. We did that to increase Figure 8 readability, although at the expense of the scientific robustness. However, after removing the adjustment, it appears that the final differences between scenarios have not changed at all. See modifications in Section 2.7 shown above.

I do not understand why constant emissions for 2000 are used? In Sect. 2.4 you note that transient emissions since 2000 are prepared. You also report figures (although averaged) for 2006-2018. What is the difference between the pairs of TOT_ and d13_ simulations? Because you state that total CH_4 is a sum of $^{13}CH_4$ and $^{12}CH_4$ in your setup, why one has to simulate TOT_ ?

We made new simulations using 2000-2018 transient emissions. The transient emissions were previously used for TOT_CHL and TOT_REF runs but we managed to merge all the isotope and non-isotope simulations to increase readability. Now, all runs start from 2000 and use 2000-2018 emissions and have different names compared to the previous version (see Table 5 below). Using 2000-2018 emissions instead of 2000 emissions did not change the differences shown in Figure 8 but slightly impacted the absolute time-series. Nevertheless, results (but not the conclusions) from Sections 3.1, 3.2, and 3.3 were impacted since all runs simulating methane mixing ratios start now in 2000 (instead of 2006).

Regarding δ^{13}C-CH_4 values and considering all the changes made in the revised paper, only the new method used to implement the soil sink in LMDz has slightly impacted the results. See modifications in Section 2.7 above and Table 5 below.

Table 1. Nomenclature and characteristics of simulations. See Sect. 3.1 for more information about the sensitivity tests.

Simulation name	Traced species	Cl-CH_4 Reaction	Simulation period	Tropospheric chlorine	MBL chlorine	Stratospheric chlorine	Decreasing chlorine
REF	$^{12}CH_4$ - $^{13}CH_4$	NO	2000-2018	X	X	X	X
Sensitivity tests							
S1	$^{12}CH_4$ - $^{13}CH_4$	YES	2000-2018	240 cm^{-3}	130 cm^{-3}	YES	NO
S2	$^{12}CH_4$ - $^{13}CH_4$	YES	2000-2018	NO	NO	YES	NO
S3	$^{12}CH_4$ - $^{13}CH_4$	YES	2000-2018	240 cm^{-3}	130 cm^{-3}	NO	NO
S4	$^{12}CH_4$ - $^{13}CH_4$	YES	2000-2018	620 cm^{-3}	335 cm^{-3}	YES	NO
S5	$^{12}CH_4$ - $^{13}CH_4$	YES	2000-2018	620 cm^{-3}	1200 cm^{-3}	YES	NO
S6	$^{12}CH_4$ - $^{13}CH_4$	YES	2000-2018	240 cm^{-3}	130 cm^{-3}	YES	5% per decade
S7	$^{12}CH_4$ - $^{13}CH_4$	YES	2000-2018	620 cm^{-3}	1200 cm^{-3}	YES	5% per decade

Did you find any effect on seasonal cycle by including Cl? The reaction with Cl possibly induces stronger seasonal cycle. It would be valuable to give discussion on this.

Looking at the seasonal cycle is indeed of interest. We analyzed the impact on seasonal cycle and included new results in Section 3.1 (P13 L8-12).

The inclusion of Cl influences the CH_4 seasonal cycle slightly at the surface but more significantly near the tropopause and above. In our model, at the surface, the seasonal cycle amplitude increases by 0.8 % - 0.9 % at global scale and by 0.8 % - 1.3 % in polar regions depending on the scenario, which is very low. Above 15 km, this increase can reach 12% at global scale and 21 % in polar regions. As expected, the most significant changes are seen above the tropopause where the Cl sink highly impacts total CH_4 removal.

---

3 Specific and technical comments

All specific and technical comments have been addressed and many modifications have been applied following the suggestions from the reviewers. We answer here to the major ones.

Is the "total" CH_4 set equal to sum of $^{13}CH_4$ and $^{12}CH_4$, or the latter are scaled up at the same ratio? This question is important for upper stratospheric budgets, where fractionation is high and mixing ratios are low. . .

Total CH_4 is set equal to the sum of $^{13}CH_4$ and $^{12}CH_4$. We actually wanted that because we think taking total CH_4 equal to $^{12}CH_4$, as it is done in some studies, could result in significant errors.

Are there no 3D model focusing on Cl impact in the stratosphere to date???

We actually did not find any. That is the main reason for making this study. We apologize if we miss some.

What is the sense of showing averages for this period? ranges would be much more useful

Could you add min. max. of the isotopic signatures for sources that varies between regions?

All this information has been added to Table 2 in the text, page 8 (or see Table 2 below).

Table 2. Annual fluxes and mean (flux- and area-weighted) isotopic signatures of methane sources averaged over 2000-2018 for multiple categories. Min and max over the time-window are displayed in brackets for anthropogenic sources that exhibits inter-annual variability. The isotopic source signatures with a * symbol are prescribed with a regional variability. The value given here is the mean over the 11 regions. Min and max are displayed in parentheses. Soil sink is included in order to compare its intensity to other categories.

Natural sources	**Annual flux** ($Tg\,yr^{-1}$)	$\delta^{13}C\text{-}CH_4$ (‰)	**Anthropogenic sources**	**Annual flux** ($Tg\,yr^{-1}$)	$\delta^{13}C\text{-}CH_4$ (‰)
Wetlands	180.2	-58.6 (-65.0/-50.0)*	Livestock	112.3 [102.2 – 120.7]	-61
Termites	8.7	-63	Rice cultivation	36.0 [32.5 - 38.8]	-63
Ocean	14.4	-42	Oil, Gas, Industry	71.2 [61.2 – 78.8]	-39.7 (-54.7/-40.7)*
Geological (onshore)	15.0	-50	Biofuels - Biomass	27.6 [23.6 – 35.5]	-25.8 (-24.9/-20.9)*
Soil	-37.9	KIE_{soil}=1.020	Waste	66.1 [59.4 – 72.9]	-49.7
			Coal	32.5 [21.9 – 38.8]	-35
Total	526.5 [483.6 - 555.2]	-51.1 [-51.6 – -50.5]			

P11L8-13: these two simulations should have different results; which are reported in this paragraph? Furthermore, what is the sense of making a simulation without Cl, when its contribution can be simply inferred from the model? Removing Cl may

shift the photochemistry of the model to much more unrealistic state, you have to show that this is not the case. I see more sense in a sensitivity simulation where CH_4+Cl reaction does not have 13C fractionation.

We agree that the first sentence is misleading as the results of Section 3.1 do not rely on differences between TOT_CHL (now S0) and TOT_REF (now REF). This sentence has been removed. As only chemical reactions are included in the model, removing Cl cannot shift the photochemistry as there is none. This study also aims at showing the impact of not including the Cl sink in a model, which many inverse modelers tend to do. Therefore, we find it more impactful to analyze a simulation without any Cl sink implemented. Here are the modifications applied to Section 3.1 (P12 L3-7).

The total stratospheric CH_4 sink is found to be 24.68 ± 0.73 (1σ for inter-annual variability) Tg yr^{-1} on average over 2000-2018 ($\sim$ 5.3 % of total atmospheric sink) in REF. The simulations yield a stratospheric Cl sink of 7.16 ± 0.27 Tg yr^{-1}, thus contributing about 29% to the total stratospheric sink. This result is at the lower end of the range estimated previously for the period 2000-2009 (Kirschke et al., 2013; Saunois et al., 2019) : [16-84] Tg yr^{-1} for total stratospheric loss with a Cl contribution between 20 and 35%.

P7L20 : Unclear sentence, you set the same (i.e. one) constant signature for all other emission categories? It is important to mention whether the signatures of compiled emissions exhibit any significant temporal trends; if there are any, perhaps they could be illustrated next to Figure S2?

We agree that this sentence was not clear, and has been corrected. We set a specific (different) signature for each category. This specific signature is set globally constant for categories that are not wetlands, gas and biofuels-biomass. Although all prescribed signatures are constant over time, flux-mean signatures are changing because some emissions exhibit temporal trends. We show source signature temporal variations in Figure S4 (Figure S2 is now Figure S3 due to modifications in the supplementary information) and modified the text as follows (P7 L27 - P8 L3):

Isotope source signatures are based on literature average values and summarized in Table 2. We use region-specific signatures over 11 regions derived from the TransCom project (see Figure S6) for wetlands, gas and biofuels-biomass categories that exhibit strong regional variabilities in signatures. A global signature value is prescribed to the other categories. All signatures are set constant over time. More information about the regional isotopic signatures and the references are provided in the supporting information (Text S1). Wetlands isotopic signatures were taken from multiple regional studies around the world and aggregated into a 11-regions map, in order to be consistent with the other categories.

P8L16-18: on which grounds you make this assumption? e.g. conditions within and outside polar vortex can vary substantially, which one would have to take into account for high-latitude stations

We understand the concern. The balloon measurement uncertainties (generally near or below 0.2 ‰ above 10km) were not included in our first version but this has been corrected. Balloon measurements were performed mainly during the 1990-2000 decade while our study starts in 2000. As a result, we use the day of year of the flight to compare with our simulated profile in year 2000 (same day of the year). Doing this introduces probably different meteorological conditions between simulations and observations. However, above 10 km altitude, simulated vertical profiles exhibit nearly no inter-annual variability and this variability is way below the measurement uncertainties. Therefore, using the year 2000 instead of the year of the measurement retrieval would not change the conclusions, especially that we are making a qualitative comparison and not a quantitative comparison. A quantitative comparison would have required an interpolation of the profiles but we are not sure of the validity and robustness of such an interpolation on δ^{13}C-CH_4 values. We included the following explanation in Section 3.4 (P18 L7-14).

Here we compare our simulated results to the observations from Röckmann et al. (2011) (Table 4). Balloon measurements were performed mainly before 2000 while our study starts in 2000. As a result, we use the day of year of the flight to compare with our simulated profile in year 2000 (same day of the year). However, above 10 km, δ^{13}C-CH_4 simulated profiles show no significant inter-annual variability during the 2000-2018 period and this variability is much smaller than the measurement uncertainties (generally below 0.2 ‰ above 10km). Therefore, using simulated results for year 2000 instead of the true year to compare observations above 10 km is valid. Implementing the Cl sink drastically improves the model-observation comparison above 10km (Figure 7), in agreement with McCarthy (2003). As a result, LMDz represents correctly the processes affecting δ^{13}C-CH_4.

P2L13: you mention mostly inverse modelling studies, however here you use forward modelling; I believe it is important to review/refer to the forward modelling studies using CH_4 isotopes, too (I can now remember only NIWA group that is missing here, e.g. Schaefer et al. (2016, doi:10.1126/science.aad2705), though there are more)

We included Schaefer et al. (2016) in the references and also added some references regarding forward modelling, see below (P2 L12-19).

As the CH_4 isotope ratio sampling network is very sparse, modelling is necessary to study $^{13}CH_4$:$^{12}CH_4$ spatio-temporal characteristics. Several studies have been trying to improve the agreement between observed and simulated δ^{13}C-CH_4 in multiple regions both in the troposphere (Warwick et al., 2016; Monteil et al., 2011; Allan et al., 2007) and stratosphere (McCarthy, 2003; Wang et al., 2002). Besides, using CH_4 mixing ratio jointly with observations of $^{13}CH_4$:$^{12}CH_4$ isotope ratio in inversions can potentially allow for source differentiation if their isotopic signature are well enough characterized (Bousquet et al., 2006). This method has already been applied in previous studies (Thompson et al., 2018; McNorton et al., 2018; Rice et al., 2016; Schaefer et al., 2016; Neef et al., 2010). However, those attempts of joint inversions do not reach the same conclusions.

P3L14: are winds nudged in the online version and then fed to the offline version of the model?.

Yes, indeed. We added a small explanation to the text. (P5 L7-10)

It is not concluded in Sect. 2.3 (P5L27-30) that the tropospheric Cl in your runs is underestimated; it is lower than in two of three studies referenced

We added a sentence specifying that we consider our tropospheric Cl values as underestimated. (P13 L2)

P15 L16-20: The sentences are not clear. You explain reduction ratio in range (%) and in absolute value (ppb), and different seasons for different layers of atmosphere. This might be more readable if consistent metric is used.

We find important to have the two metrics to see the differences of impact between the troposphere and the stratosphere. For the troposphere, the reduction ratio is large but the raw difference value is small. Stratosphere have opposite results. However, we agree the sentences were not clear and we tried to improve the readability. Below are the modifications in Section 3.3 (P14 L9 - P15 L8):

We compute the difference between simulated and observed profiles after the simulated values have been linearly interpolated on the associated AirCore profile pressure axis. Points outside the data range were extrapolated using the inferred interpolation function. Model-observation discrepancy distributions are shifted to smaller values (reduction ratio smaller than 100 %) when including the Cl sink for all seasons in both the troposphere and stratosphere (Fig. 5). This illustrates some modelling improvement when including Cl. We find that the implementation of Cl sink reduces the difference between simulated and observed vertical profiles on average by 31.7 ± 13.2 % (1σ for intra-profile variability) in the stratosphere over the entire dataset and by 59.3 ± 24.8 % in the troposphere. This ratio represents a CH_4 reduction of about 27 ppb in the stratosphere and 9 ppb in the troposphere. Although the Cl sink is included, simulations show significant remaining discrepancies in the troposphere compared to AirCore CH_4 observations ($\sim$20 ppb, 1.1% of the tropospheric mixing ratio) and in the stratosphere ($\sim$85 ppb, 5.5% of the stratospheric mass-weighted mean mixing ratio).

P15 L28-29: "Those may be induced by small scale filaments of methane coming from polar regions, that cannot be adequately reproduced by our low-resolution model and seasonal averaging." This can be checked with meteorological data.

We actually looked at outputs from the Monitoring Atmospheric Composition and Climate (MACC) project (Marécal et al., 2015) to make this assumption. We added this explanation to the text. See next question to see the modified Section 3.3 (P16 L4-6).

What do you mean by "small variations"? Variations as std, or differences from the observations?

"Small variations" was not an adequate formulation. It refers to the localized peaks of methane mixing ratio that can be seen in observed vertical profiles near the tropopause, mostly during the MAM season. We changed the formulation by using "localized spikes". Below are the modifications in Section 3.3 (P15 L34 - P16 L6):

Figure 6 displays the comparison between AirCore observations and associated simulated profiles (with Cl sink) linearly interpolated on a regular altitude axis following the same method as before. Above the tropopause between 15-25 km, the model-observation difference can exceed 150 ppb on average during spring and summer even with Cl sink. All the profiles and their associated simulated profiles are plotted in Figure S5. A closer analysis of individual profiles shows that very localized mixing ratio spikes occur more often during spring and summer than during other seasons, especially around the tropopause. Additionally, inversions of mixing ratios can occur above the tropopause. After analyzing outputs from the Monitoring Atmospheric Composition and Climate (MACC) project (Marécal et al., 2015), those are likely to be induced by small scale filaments of either high or low CH_4 coming from polar regions, that cannot be adequately reproduced by our low-resolution model.

P20 L15-16: The impact is actually on the forward run, which then influences the inversion results on flux estimates. In addition, the value "0.27 ‰ is dependent on model and its setups, but the sentence is phrased as if it it a general statement. Please consider rephrasing.

We agree. We removed the sentence and modified a sentence in the conclusion (P22 L11-14):

In addition, the stratospheric impact of Cl on surface δ^{13}C-CH_4 values was found to be as high as 0.25 ‰ with our model and the associated setup, and hence of the same magnitude as recorded variations of δ^{13}C-CH_4 in the past decade. However, the recent decrease in Cl concentration in the stratosphere owing to the Montreal Protocol is not likely an explanation for the recent shift of δ^{13}C-CH_4 values towards more negative values.

The observed seasonal cycle amplitude presented in the figure is much smaller than those modelled, but "std" of the observations show clear seasonal cycle. Did you use different averaging for model and observed values? In addition, it might be better to present figure with two panels, one on deseasonalised trends and another for monthly values.

We are not sure to fully understand this comment as the seasonal cycle is well reproduced by the simulations. The averaging method is exactly the same. Simulated values are taken at available sites and aggregated the same way as the observed values. To increase clarity, we removed the "std" as it does not bring any additional scientific value to the Figure 8. As suggested by Reviewer #1, we presented the Figure 8 with two panels, another for monthly values (left) and one for deseasonalised trends (right), see Figure 1 below.

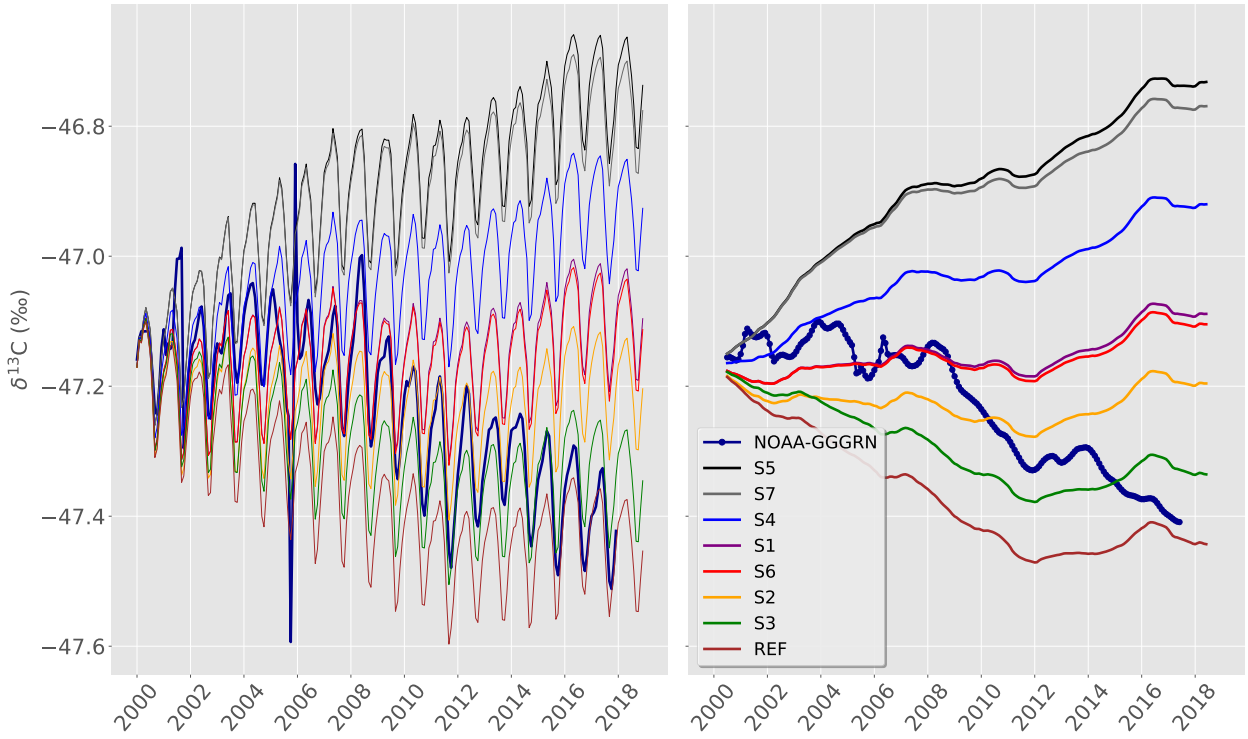

Figure 1. Time series of surface δ^{13}C-CH_4 global mean value for multiple scenarios. The left panel shows the observed and simulated monthly values. The right panel displays the associated deseasonalized trends. The globally-averaged NOAA-GGGRN δ^{13}C-CH_4 record is in dark blue. Only MBL sites (i.e. samples from the site are predominantly of well-mixed MBL air) are used here. Extreme values in 2001 and 2005 are explained by a lack of monthly values either in the North (2001-09, 2005-12) or the South Hemisphere (2001-06, 2001-07, 2005-10, 2005-11). However, this lack of data cannot explain the peak in 2008.

P18 L10 – P19 L2: This explanation is better fit to the method section.

Section 2.3: First two paragraphs can be in Introduction, as this does not describe “method”.

P21 L17-L28: Please move this to earlier section, and only include some summary on this in the Conclusion.

We agree and followed those suggestions.

Figure 4 caption: – What is (a) in “Dry-air column average mole fraction of methane (a) and differences”? – I assume a) and b) are for the total column. Please specify. – Add “from” in a) before the name of the simulation, i.e. “average mole fraction of methane from TOT_CHL”

The (a) was referring to the panel (a), i.e. the upper-left panel that has an "a)" displayed in white font in it. We changed the caption to make it clearer.

References

Allan, W., Struthers, H., and Lowe, D. C.: Methane carbon isotope effects caused by atomic chlorine in the marine boundary layer: Global model results compared with Southern Hemisphere measurements, Journal of Geophysical Research, 112, https://doi.org/10.1029/2006JD007369, http://doi.wiley.com/10.1029/2006JD007369, 2007.

Bousquet, P., Ciais, P., Miller, J. B., Dlugokencky, E. J., Hauglustaine, D. A., Prigent, C., Van der Werf, G. R., Peylin, P., Brunke, E.-G., Carouge, C., Langenfelds, R. L., Lathière, J., Papa, F., Ramonet, M., Schmidt, M., Steele, L. P., Tyler, S. C., and White, J.: Contribution of anthropogenic and natural sources to atmospheric methane variability, Nature, 443, 439–443, https://doi.org/10.1038/nature05132, http://www.nature.com/articles/nature05132, 2006.

Folberth, G. A., Hauglustaine, D. A., Lathière, J., and Brocheton, F.: Interactive chemistry in the Laboratoire de Météorologie Dynamique general circulation model: model description and impact analysis of biogenic hydrocarbons on tropospheric chemistry, Atmospheric Chemistry and Physics, 6, 2273–2319, https://doi.org/10.5194/acp-6-2273-2006, http://www.atmos-chem-phys.net/6/2273/2006/, 2006.

Hauglustaine, D. A., Hourdin, F., Jourdain, L., Filiberti, M.-A., Walters, S., Lamarque, J.-F., and Holland, E. A.: Interactive chemistry in the Laboratoire de Météorologie Dynamique general circulation model: Description and background tropospheric chemistry evaluation, Journal of Geophysical Research: Atmospheres, 109, https://doi.org/10.1029/2003JD003957, https://agupubs.onlinelibrary.wiley.com/doi/full/10.1029/2003JD003957, 2004.

Kirschke, S., Bousquet, P., Ciais, P., Saunois, M., Canadell, J. G., Dlugokencky, E. J., Bergamaschi, P., Bergmann, D., Blake, D. R., Bruhwiler, L., Cameron-Smith, P., Castaldi, S., Chevallier, F., Feng, L., Fraser, A., Heimann, M., Hodson, E. L., Houweling, S., Josse, B., Fraser, P. J., Krummel, P. B., Lamarque, J.-F., Langenfelds, R. L., Le Quéré, C., Naik, V., O'Doherty, S., Palmer, P. I., Pison, I., Plummer, D., Poulter, B., Prinn, R. G., Rigby, M., Ringeval, B., Santini, M., Schmidt, M., Shindell, D. T., Simpson, I. J., Spahni, R., Steele, L. P., Strode, S. A., Sudo, K., Szopa, S., van der Werf, G. R., Voulgarakis, A., van Weele, M., Weiss, R. F., Williams, J. E., and Zeng, G.: Three decades of global methane sources and sinks, Nature Geoscience, 6, 813–823, https://doi.org/10.1038/ngeo1955, http://www.nature.com/articles/ngeo1955, 2013.

Locatelli, R., Bousquet, P., Saunois, M., Chevallier, F., and Cressot, C.: Sensitivity of the recent methane budget to LMDz sub-grid-scale physical parameterizations, Atmospheric Chemistry and Physics, 15, 9765–9780, https://doi.org/10.5194/acp-15-9765-2015, http://www.atmos-chem-phys.net/15/9765/2015/, 2015.

Marécal, V., Peuch, V.-H., Andersson, C., Andersson, S., Arteta, J., Beekmann, M., Benedictow, A., Bergström, R., Bessagnet, B., Cansado, A., Chéroux, F., Colette, A., Coman, A., Curier, R. L., Denier van der Gon, H. a. C., Drouin, A., Elbern, H., Emili, E., Engelen, R. J., Eskes, H. J., Foret, G., Friese, E., Gauss, M., Giannaros, C., Guth, J., Joly, M., Jaumouillé, E., Josse, B., Kadygrov, N., Kaiser, J. W., Krajsek, K., Kuenen, J., Kumar, U., Liora, N., Lopez, E., Malherbe, L., Martinez, I., Melas, D., Meleux, F., Menut, L., Moinat, P., Morales, T., Parmentier, J., Piacentini, A., Plu, M., Poupkou, A., Queguiner, S., Robertson, L., Rouïl, L., Schaap, M., Segers, A., Sofiev, M., Tarasson, L., Thomas, M., Timmermans, R., Valdebenito, , van Velthoven, P., van Versendaal, R., Vira, J., and Ung, A.: A regional air quality forecasting system over Europe: the MACC-II daily ensemble production, Geoscientific Model Development, 8, 2777–2813, https://doi.org/https://doi.org/10.5194/gmd-8-2777-2015, https://www.geosci-model-dev.net/8/2777/2015/, 2015.

McCarthy, M. C.: Carbon and hydrogen isotopic compositions of stratospheric methane: 2. Two-dimensional model results and implications for kinetic isotope effects, Journal of Geophysical Research, 108, https://doi.org/10.1029/2002JD003183, http://doi.wiley.com/10.1029/2002JD003183, 2003.

McNorton, J., Wilson, C., Gloor, M., Parker, R. J., Boesch, H., Feng, W., Hossaini, R., and Chipperfield, M. P.: Attribution of recent increases in atmospheric methane through 3-D inverse modelling, Atmospheric Chemistry and Physics, 18, 18 149–18 168, https://doi.org/https://doi.org/10.5194/acp-18-18149-2018, https://www.atmos-chem-phys.net/18/18149/2018/, 2018.

Monteil, G., Houweling, S., Dlugockenky, E. J., Maenhout, G., Vaughn, B. H., White, J. W. C., and Rockmann, T.: Interpreting methane variations in the past two decades using measurements of CH_4 mixing ratio and isotopic composition, Atmospheric Chemistry and Physics, 11, 9141–9153, https://doi.org/https://doi.org/10.5194/acp-11-9141-2011, https://www.atmos-chem-phys.net/11/9141/2011/acp-11-9141-2011.html, 2011.

Neef, L., Weele, M. v., and Velthoven, P. v.: Optimal estimation of the present-day global methane budget, Global Biogeochemical Cycles, 24, https://doi.org/10.1029/2009GB003661, https://agupubs.onlinelibrary.wiley.com/doi/abs/10.1029/2009GB003661, 2010.

Rice, A. L., Butenhoff, C. L., Teama, D. G., Röger, F. H., Khalil, M. A. K., and Rasmussen, R. A.: Atmospheric methane isotopic record favors fossil sources flat in 1980s and 1990s with recent increase, Proceedings of the National Academy of Sciences, 113, 10 791–10 796, https://doi.org/10.1073/pnas.1522923113, https://www.pnas.org/content/113/39/10791, 2016.

Röckmann, T., Brass, M., Borchers, R., and Engel, A.: The isotopic composition of methane in the stratosphere: high-altitude balloon sample measurements, Atmospheric Chemistry and Physics, 11, 13 287–13 304, https://doi.org/https://doi.org/10.5194/acp-11-13287-2011, https://www.atmos-chem-phys.net/11/13287/2011/, 2011.

Saunois, M., Stavert, A. R., Poulter, B., Bousquet, P., Canadell, J. G., Jackson, R. B., Raymond, P. A., Dlugokencky, E. J., Houweling, S., Patra, P. K., Ciais, P., Arora, V. K., Bastviken, D., Bergamaschi, P., Blake, D. R., Brailsford, G., Bruhwiler, L., Carlson, K. M., Carrol, M., Castaldi, S., Chandra, N., Crevoisier, C., Crill, P. M., Covey, K., Curry, C. L., Etiope, G., Frankenberg, C., Gedney, N., Hegglin, M. I., Höglund-Isakson, L., Hugelius, G., Ishizawa, M., Ito, A., Janssens-Maenhout, G., Jensen, K. M., Joos, F., Kleinen, T., Krummel, P. B., Langenfelds, R. L., Laruelle, G. G., Liu, L., Machida, T., Maksyutov, S., McDonald, K. C., McNorton, J., Miller, P. A., Melton, J. R., Morino, I., Müller, J., Murgia-Flores, F., Naik, V., Niwa, Y., Noce, S., O'Doherty, S., Parker, R. J., Peng, C., Peng, S., Peters, G. P., Prigent, C., Prinn, R., Ramonet, M., Regnier, P., Riley, W. J., Rosentreter, J. A., Segers, A., Simpson, I. J., Shi, H., Smith, S. J., Steele, P. L., Thornton, B. F., Tian, H., Tohjima, Y., Tubiello, F. N., Tsuruta, A., Viovy, N., Voulgarakis, A., Weber, T. S., van Weele, M., van der Werf, G. R., Weiss, R. F., Worthy, D., Wunch, D., Yin, Y., Yoshida, Y., Zhang, W., Zhang, Z., Zhao, Y., Zheng, B., Zhu, Q., Zhu, Q., and Zhuang, Q.: The Global Methane Budget 2000–2017, Earth System Science Data Discussions, pp. 1–138, https://doi.org/10.5194/essd-2019-128, https://www.earth-syst-sci-data-discuss.net/essd-2019-128/, 2019.

Schaefer, H., Fletcher, S. E. M., Veidt, C., Lassey, K. R., Brailsford, G. W., Bromley, T. M., Dlugokencky, E. J., Michel, S. E., Miller, J. B., Levin, I., Lowe, D. C., Martin, R. J., Vaughn, B. H., and White, J. W. C.: A 21st-century shift from fossil-fuel to biogenic methane emissions indicated by 13CH4, Science, 352, 80–84, https://doi.org/10.1126/science.aad2705, https://science-sciencemag-org.insu.bib.cnrs.fr/content/352/6281/80, 2016.

Snover, A. K. and Quay, P. D.: Hydrogen and carbon kinetic isotope effects during soil uptake of atmospheric methane, Global Biogeochemical Cycles, 14, 25–39, https://doi.org/10.1029/1999GB900089, https://agupubs.onlinelibrary.wiley.com/doi/abs/10.1029/1999GB900089, 2000.

Thompson, R. L., Nisbet, E. G., Pisso, I., Stohl, A., Blake, D., Dlugokencky, E. J., Helmig, D., and White, J. W. C.: Variability in Atmospheric Methane From Fossil Fuel and Microbial Sources Over the Last Three Decades, Geophysical Research Letters, 45, 11,499–11,508, https://doi.org/10.1029/2018GL078127, https://agupubs.onlinelibrary.wiley.com/doi/abs/10.1029/2018GL078127, 2018.

Wang, J. S., McElroy, M. B., Spivakovsky, C. M., and Jones, D. B. A.: On the contribution of anthropogenic Cl to the increase in ^{13}C of atmospheric methane: ANTHROPOGENIC Cl AND ^{13}C OF METHANE, Global Biogeochemical Cycles, 16, 20–1–20–11, https://doi.org/10.1029/2001GB001572, http://doi.wiley.com/10.1029/2001GB001572, 2002.

Warwick, N. J., Cain, M. L., Fisher, R., France, J. L., Lowry, D., Michel, S. E., Nisbet, E. G., Vaughn, B. H., White, J. W. C., and Pyle, J. A.: Using delta13C-CH4 and deltaD-CH4 to constrain Arctic methane emissions, Atmospheric Chemistry and Physics, 16, 14 891–14 908, https://doi.org/10.5194/acp-16-14891-2016, http://www.atmos-chem-phys.net/16/14891/2016/, 2016.

Impact of atomic chlorine on the modelling of total methane and its ^{13}C~~C~~CH$_4$:^{12}C ~~isotopic~~ CH$_4$ isotope ratio at global scale

Joël Thanwerdas[1,*], Marielle Saunois[1], Antoine Berchet[1], Isabelle Pison[1], Didier Hauglustaine[1], Michel Ramonet[1], Cyril Crevoisier[2], Bianca Baier[3,4], Colm Sweeney[4], and Philippe Bousquet[1]

[1]Laboratoire des Sciences du Climat et de l'Environnement, CEA-CNRS-UVSQ, IPSL, Gif-sur-Yvette, France.
[2]Laboratoire de Météorologie Dynamique, École Polytechnique, IPSL, Palaiseau, France.
[3]Cooperative Institute for Research in Environmental Sciences (CIRES), University of Colorado-Boulder, Boulder, CO, USA 80305
[4]NOAA Earth System Research Laboratory Global Monitoring Division, Boulder, CO, USA 80305

Correspondence: J. Thanwerdas (joel.thanwerdas@lsce.ipsl.fr)

Abstract.

Methane (CH_4) is the second strongest anthropogenic greenhouse gas after carbon dioxide (CO_2) and is responsible for about 20% of the warming induced by long-lived greenhouse gases since pre-industrial times. Oxidation by the hydroxyl radical (OH) is the dominant atmospheric sink for methane, contributing to approximately 90% of ~~the~~ total methane loss. Chemical losses by reaction with atomic oxygen (O^1D) and chlorine radicals (Cl) in the stratosphere ~~are other sinks, contributing~~ contribute about 3% to the ~~total~~ methane destruction. ~~Moreover~~Additionally, the reaction with Cl is very fractionating, ~~thus~~ i.e. reacting faster with $^{12}CH_4$ than with $^{13}CH_4$. Therefore, it has a much larger impact on δ^{13}C-CH_4 than ~~the reaction with OH~~ OH oxidation. In this paper, we assess the impact of ~~atomic Cl~~ Cl oxidation on atmospheric methane mixing ratios, methane atmospheric loss and atmospheric δ^{13}C-CH_4. The offline version of the ~~Global~~ 3-D General Circulation Model (GCM) LMDz, coupled to a chemistry module including ~~the major methane chemical reactions~~all relevant methane chemical sinks, is run to simulate CH_4 concentrations and δ^{13}C-CH_4 at the global scale. ~~Atmospheric~~ The mean atmospheric methane sink by Cl atoms in the stratosphere is found to be 7.32 ± 0.16 Tg/yr over the 2000-2018 period using a climatological (2003-2009 average) Cl field. Methane observations from vertical profiles obtained using AirCore samplers ~~above~~ at 11 different locations ~~across the globe~~ worldwide and balloon measurements of δ^{13}C-CH_4 ~~and methane~~ isotopic ratios and CH_4 mixing ratios are used to assess the impact of ~~the~~ Cl sink in ~~the chemistry transport model~~LMDz. Above 10 km, ~~the presence of~~ adding Cl in the model ~~is found to have~~ has only a small impact on the ~~vertical profile of total methane~~ CH_4 vertical profile but a major influence on δ^{13}C-CH_4 values, significantly improving the agreement between simulations and available observations of δ^{13}C-CH_4. Stratospheric Cl ~~is also found~~ appears to have a substantial impact on surface δ^{13}C-CH_4 values, leading to a difference of + ~~0.27~~ 0.25 ‰ (~~less negative values~~hence enriched with $^{13}CH_4$) after a 19-year run ~~.~~ spanning 2000 to 2018. As a result, this study suggests that the Cl sink needs to be properly taken into account (magnitude and trends) in order to better understand trends in the atmospheric δ^{13}C-CH_4 signal when using forward or inverse simulations of atmospheric chemistry transport models~~for forward or inverse calculations~~.

1 Introduction

Methane (CH_4) is the second most powerful anthropogenic greenhouse gas after carbon dioxide (CO_2) and has a strong impact both on tropospheric and stratospheric chemistry. Its ~~globally averaged~~ atmospheric concentrations have almost tripled since pre-industrial times (Etheridge et al., 1998), exceeding ~~1850 ppb in 2017.~~ 1860 ppb in 2019. The growth rate slowed in the 1990s and stabilized between 1999 and 2006. However, ~~methane concentrations resumed increasing~~ CH_4 concentrations resumed increase after 2006 and are still growing since then (Nisbet et al., 2019).

Due to large uncertainties in the estimation of ~~methane~~ CH_4 sources and sinks (Saunois et al., 2016), the causes of this continued increase in 2006 remain controversial (Saunois et al., 2017; Turner et al., 2019). Many studies used an inversion framework to optimize ~~the~~ CH_4 sources and sinks ~~in order to match atmospheric observations using the total methane information alone~~ using CH_4 concentrations as a constraint (Bergamaschi et al., 2018; Locatelli et al., 2015a). However, ~~total~~ CH_4 ~~mole fractions~~ mixing ratios provide insufficient information to determine effectively the causes of this increase (Saunois et al., 2017). The ^{13}~~C~~CH_4:^{12}~~C isotopic methane ratio~~ CH_4 methane isotope ratio, on the contrary, can be a powerful additional constraint to characterize a given ~~methane source. For instance, analyzing~~ CH_4 source. Analyzing the recent shift of this ratio to more negative values, ~~(Nisbet et al., 2016, 2019)~~ Nisbet et al. (2016, 2019) suggested that the ~~methane increase~~ increase in CH_4 mixing ratios since 2006 is driven by an increase in biogenic ~~methane emissions. Using total~~ CH_4 emissions. As the CH_4 isotope ratio sampling network is very sparse, modelling is necessary to study $^{13}CH_4$:$^{12}CH_4$ spatio-temporal characteristics. Several studies have been trying to improve the agreement between observed and simulated δ^{13}C-CH_4 in multiple regions both in the troposphere (Warwick et al., 2016; Monteil et al., 2011; Allan et al., 2007) and stratosphere (McCarthy, 2003; Wang et al., 2002). Besides, using CH_4 mixing ratio jointly with observations of ^{13}~~C~~CH_4:^{12}~~C~~ CH_4 isotope ratio in inversions can potentially allow ~~us to differentiate sources~~ for source differentiation if their isotopic signature ~~can be characterized well enough~~ are well enough characterized (Bousquet et al., 2006). This method has already been ~~used~~ applied in previous studies ~~(Thompson et al., 2018; McNorton~~ (Thompson et al., 2018; McNorton et al., 2018; Rice et al., 2016; Schaefer et al., 2016; Neef et al., 2010). However, those attempts of joint inversions do not reach ~~exactly~~ the same conclusions. ~~Indeed, many~~ Many parameters may influence the ^{13}~~C~~CH_4:^{12}~~C~~ CH_4 ratio such as ~~the~~ kinetic isotope effects associated with ~~the sinks or the source isotopic signatures. The uncertainties and the~~ sinks or isotopic source signatures ($\delta^{13}C_{source}$). First, uncertainties and regional variability of ~~the isotopic signatures is an issue that should not be disregarded~~ isotopic signatures should be considered rigorously (Feinberg et al., 2018), especially for wetlands (Ganesan et al., 2018) ~~that~~ which account for about 30~~% of the~~ % of total source and exhibit a distinctively light signature (depleted in $^{13}CH_4$) and a strong regional variability in isotope composition. In addition, ~~due to the fractionation potential of chemical reactions in the atmosphere (McCarthy, 2003; Saueressig et al., 2001),~~ the atmospheric isotopic ratio is largely affected by the intensity of the ~~main sinks~~ major sinks due to the fractionation potential (namely, having distinct reaction rates depending on the isotope) of chemical reactions in the atmosphere (McCarthy, 2003; Saueressig et al., 2001).

Three atmospheric species contribute to ~~methane~~ CH_4 removal in the ~~atmosphere : the hydroxyl radical~~ troposphere and stratosphere : hydroxyl radicals (OH), electronically excited atomic oxygen atoms (O^1D) and ~~the Cl radical~~ Cl radicals (Cl).

Oxidation by OH is the dominant sink and is responsible for about 90% of ~~the total methane~~ CH_4 loss (Saunois et al., 2016). The reactions $CH_4 + O(^1D)$ and CH_4 + Cl, also contribute substantially to ~~methane~~ CH_4 removal, especially in the stratosphere where $O(^1D)$ and Cl atoms are found in larger amounts than in the troposphere. Besides, the ~~exceptionally large isotope fractionation in the~~ reaction CH_4 + Cl exhibits an exceptionally large isotopic fractionation (1.066 compared ~~with~~ to 1.0039 for CH_4 + OH in this paper, see Sect. 2.2) ~~implies~~ and induces a significant effect on ^{13}~~C~~CH_4:^{12}~~C isotopic~~ CH_4 isotope ratio values.

Tropospheric and stratospheric Cl have different origins. Tropospheric Cl originates mostly from sea salt, organochlorines and open fires (Wang et al., 2019; Hossaini et al., 2016). The most important inorganic Cl compound in the troposphere is hydrogen chlorine (HCl). Its principal source is acid displacement from sea salt aerosol. HCl is quickly removed from the troposphere by wet deposition due to its high solubility in water. Hence, it is not the main source of stratospheric Cl. The majority of Cl found above the tropopause is released from long-lived Cl containing species. Man-made organochlorines such as chlorofluorocarbons (CFCs) and hydrochlorofluorocarbons (HCFCs) (Von Clarmann, 2013; Nassar et al., 2006), along with methyl chloroform (CH_3CCl_3) and carbon tetrachloride (CCl_4), represent about 80 % of the source of Cl in the stratosphere. The rest (15-20 %) comes from methylchloride (CH_3Cl), which is mostly natural. The most abundant CFCs and HCFCs found in the stratosphere are currently CFC-11, CFC-12, CFC-113 and HCFC-22. These compounds release reactive Cl by photolysis or oxidation in the stratosphere and mesosphere. The two main Cl reservoir species in the stratosphere are HCl and chlorine nitrate ($ClONO_2$). Atomic Cl is converted to HCl mainly through the reaction with CH_4 (R2 presented below). Since the 1987 Montreal Protocol, a decline in emissions of anthropogenic long-lived Cl-containing species and consequently in HCl mixing ratios in the stratosphere have been observed (Bernath and Fernando, 2018).

The impact of Cl (on ~~methane as well as on~~ ^{13}~~C:^{12}C isotopic ratio~~ CH_4 mixing ratio and isotope ratios) has already been thoroughly studied both in the troposphere and ~~in the~~ Marine Boundary Layer (MBL) (Wang et al., 2019; Hossaini et al., 2016; Allan et al., 2007; Allan, 2005; Wang et al., 2002; Allan et al., 2001). The Cl sink was found to account for 10% to more than 20% of total boundary layer ~~methane oxidation and for~~ CH_4 oxidation and 1% to 2.5% of total CH_4 oxidation. However, Gromov et al. (2018) ~~suggest~~ suggested that the effect of Cl is highly overestimated in ~~some~~ tropospheric studies. Assessing an impact ~~from Cl~~ of Cl on CH_4 removal in the stratosphere was already attempted ~~(Röckmann et al., 2004; McCarthy, 2003; McCarthy et al., 200~~ ~~using~~ using box or 2-D ~~modelling~~models (Röckmann et al., 2004; McCarthy, 2003; Wang et al., 2002; McCarthy et al., 2001; Saueress . Here we use a 3-D chemistry transport model to quantify ~~methane~~ CH_4 loss through Cl oxidation, and to quantify the impact of atomic Cl in the stratosphere on global CH_4 ~~concentrations~~mixing ratios, XCH_4 column and ^{13}~~C~~CH_4:^{12}~~C~~ CH_4 ratio using newly available 3-D Cl fields. A set of 115 vertical profiles of total ~~methane~~ CH_4 retrieved during the 2010-2018 period using the AirCore technique (Karion et al., 2010) at 11 different locations ~~across the globe~~ worldwide are used to ~~assess potential improvements~~compare our model results, especially in the stratosphere. The ~~observations used for~~ ^{13}~~C~~CH_4:^{12}~~C isotopic ratio comparison are~~ CH_4 isotopic ratio is compared with balloon measurements presented in Röckmann et al. (2011).

Section 2 presents the model and data used to run the simulations~~as well as observations~~. In Section 3, we analyse first the impact of Cl on ~~the total methane~~ total CH_4 mixing ratios and then on ~~methane~~ the CH_4 isotopic ratio. Section 4 presents ~~a discussion and conclusions.~~

conclusions.

2 Methods

2.1 The chemistry-transport model (CTM)

The LMDz ~~Global~~ General Circulation Model (GCM) is the atmospheric component of the Institut Pierre-Simon Laplace Coupled Model (IPSL-CM) developed at the Laboratoire de Météorologie Dynamique (LMD) (Hourdin et al., 2006). The version of LMDz ~~we use~~ used is an 'offline' version dedicated to the inversion framework created by Chevallier et al. (2005): precomputed meteorological fields provided by the online version of LMDz are given as inputs to the model, ~~reducing significantly~~ significantly reducing the computational time. The model is set up at a horizontal resolution of 3.8° x 1.9° (96 grid cells in longitude and latitude) with 39 hybrid sigma-pressure levels reaching an altitude up to about 75 km. About 20 levels are dedicated to the stratosphere and the mesosphere. The model time-step is 30 min and the output ~~concentrations~~ mixing ratios are 3-hourly averaged. The horizontal winds ~~are~~ were nudged towards ECMWF meteorological analyses (ERA-Interim) in the online version of the model in order to more realistically reproduce the actual meteorology. Vertical diffusion is parameterized by a local approach from ~~Louis (1979)~~Louis (1979), and deep convection processes are parameterized by the ~~Tiedtke (1989)~~ Tiedtke (1989) scheme.

The LMDz offline model, coupled with the ~~SACS (~~Simplified Atmospheric Chemistry System (SACS) module (Pison et al., 2009), was previously used to simulate atmospheric ~~concentrations of trace gas such as methane~~mixing ratios of trace gases such as CH_4, carbon monoxide (CO), methyl-chloroform (MCF), formaldehyde (CH_2O) or dihydrogen (H_2)~~mixing ratios~~. For the purpose of this study, a new chemistry parsing system was developed (therefore replacing SACS) following the principle of the chemistry parsing system in the regional model CHIMERE (Menut et al., 2013), allowing ~~to provide~~ for user-specific governing system of chemistry reactions, thus generalizing the SACS module to any possible set of reactions. Each reaction is bound to a reaction type (simplified Arrhenius, complete Arrhenius, relative pressure, photolysis...) providing a way to compute the kinetic rate coefficients ~~which~~ that depend on temperature and pressure. The algorithm updates ~~the simulated species concentrations~~ simulated species mixing ratios at each time step ~~according to~~ following the reactions provided. The different species are either prescribed (here OH, $O(^1D)$ and Cl) or simulated. The prescribed species are not transported in LMDz, nor ~~their concentrations are updated depending on~~ are their mixing ratios updated through chemical production or destruction. ~~They~~ Such species are only used to calculate reaction rates to update simulated species at each model time step. In this study, the isotopologues $^{12}CH_4$ and $^{13}CH_4$ ~~of methane were~~ are simulated as separate tracers. Cl + CH_4 oxidation has also been implemented to complete the chemical removal of ~~methane~~CH_4, which was ~~accounted for only~~ previously only accounted for by OH + CH_4 and $O(^1D)$ + CH_4 in the SACS scheme. Here, CH_4 and its isotopologues are simulated, and OH, $O(^1D)$ and Cl distributions are prescribed from the INCA [INteraction with Chemistry and Aerosols] model (Hauglustaine et al., 2004) (see Sect. 2.3). In this study, we address ~~here~~ the sensitivity of CH_4 and its ~~isotopologues~~ isotopic ratio to the presence of Cl through forward-modeling.

2.2 Reactions with OH, O(^{1}D) and Cl and ~~Kinetic Isotope Effect~~isotope fractionation

~~Methane~~ CH_4 is removed from the ~~atmosphere through~~ troposphere and the stratosphere through the following chemical reactions with OH, O(^{1}D) and Cl:

$$CH_4 + OH^\bullet \rightarrow CH_3^\bullet + H_2O \quad \text{(R1)}$$

$$CH_4 + Cl^\bullet \rightarrow CH_3^\bullet + HCl \quad \text{(R2)}$$

$$CH_4 + O(^1D)^\bullet \rightarrow CH_3^\bullet + OH^\bullet \quad \text{(R3)}$$

$$CH_4 + O(^1D)^\bullet \rightarrow H_2 + CH_2O \quad \text{(R4)}$$

~~OH is the main sink of methane, accounting for about 90% of total methane removal. The effect of Cl and O(^{1}D) on total methane removal is significant only in the stratosphere.~~ Due to the Kinetic Isotope Effect (KIE), ~~the reaction rate coefficient associated with the reaction between methane~~ reaction rates associated with reactions between CH_4 and one of the three oxidants ~~can vary~~ above varies from one isotope to another. The KIE is defined by :

$$KIE = \frac{k_{12}}{k_{13}} \quad (1)$$

k_{12} and k_{13} denote the reaction rates for the reactions involving ~~respectively~~ $^{12}CH_4$ and $^{13}CH_4$, respectively. KIE values are usually greater than 1, ~~meaning that~~ i.e. the oxidant reacts faster with the lighter isotope. ~~The reaction rates~~ Reaction constants in this paper are taken from Burkholder et al. (2015) and ~~the~~ KIEs from Saueressig et al. (1995) for the reaction with Cl and from Saueressig et al. (2001) for reactions with OH and O(^{1}D). All ~~the reactions~~ reaction constants and associated values are reported in the Table 1. Few studies have focused on assessing ~~the KIE for~~ KIEs associated with CH_4 chemical sinks (especially for O(^{1}D) and Cl) within a wide temperature range and ~~large~~ thus significant uncertainties still remain. ~~McCarthy (2003) suggests to use those values for stratospheric methane simulations~~We chose the KIE values from Saueressig et al. (2001) and Saueressig et al. (1995) since they indicate that this data is of considerably higher precision and experimental reproductibility than earlier studies.

Table 1. ~~Rate~~ Reaction constants and KIEs of ~~the methane~~ CH_4 chemical sinks.

Reactions	KIE	Reference	Reaction constant	Reference
OH	1.0039	Saueressig et al. (2001)	$2.45 \times 10^{-12} \cdot \exp(-1775/T)$	Burkholder et al. (2015)
O(^{1}D) - R3	1.013	Saueressig et al. (2001)	1.125×10^{-10}	Burkholder et al. (2015)
O(^{1}D) - R4	1.013	Saueressig et al. (2001)	3.75×10^{-11}	Burkholder et al. (2015)
Cl	$1.043 \cdot \exp(6.455/T)$	Saueressig et al. (1995)	$7.1 \times 10^{-12} \cdot \exp(-1280/T)$	Burkholder et al. (2015)

~~Besides chemical removals, CH_4 soil uptake sink is accounted in this study as a negative source and its KIE is used to define an effective isotopic signature (see Sect. 2.5).~~

2.3 Atomic Cl field

~~Tropospheric and stratospheric Cl have different origins. Tropospheric Cl originates mostly from sea salt, organochlorines and open fires (Wang et al., 2019; Hossaini et al., 2016). The most important inorganic Cl compound in the troposphere is hydrogen chlorine (HCl). Its principal source is acid displacement from sea salt aerosol. HCl is quickly removed from the troposphere by wet deposition due to its high solubility in water. Hence, it is not the main source of stratospheric Cl. The majority of the Cl found above the tropopause is released from long-lived Cl containing species. Man-made organochlorines such as chlorofluorocarbons (CFCs) and hydrochlorofluorocarbons (HCFCs) (Von Clarmann, 2013; Nassar et al., 2006) along with methyl chloroform (CH_3CCl_3) and carbon tetrachloride (CCl_4) represent about 80 % of the source of Cl in the stratosphere. The rest (15-20 %) comes from methylchloride (CH_3Cl) which is mostly natural. The most abundant CFCs and HCFCs found in the stratosphere are currently CFC-11, CFC-12, CFC-113 and HCFC-22. These compounds release reactive Cl by photolysis or oxidation in the stratosphere and mesosphere. The two main Cl reservoir species in the stratosphere are HCl and chlorine nitrate ($ClONO_2$). Atomic Cl is converted to HCl mainly through the reaction with CH_4 (R2).~~

~~Since the 1987 Montreal Protocol, a decline in the emissions of anthropogenic long-lived Cl-containing species and consequently of the HCl concentrations in the stratosphere have been observed Bernath and Fernando, 2018.~~

~~We use the LMDz-INCA model to simulate beforehand the~~ The three-dimensional and time-dependent oxidant concentration fields (OH, O(^{1}D) and Cl ~~three-dimensional and time dependant concentrations to be prescribed in our methane simulations. LMDz-INCA couples the~~ were simulated by the LMDz GCM (described in Section 2.1) coupled to the chemistry scheme INCA [INteraction with Chemistry and Aerosols] (Folberth et al., 2006; Hauglustaine et al., 2004)~~and the LMDz GCM described in Section 2.1~~. The mass fluxes used in the offline version of LMDz were calculated by the online version of LMDz nudged to the same meteorological data. Seventeen ozone-depleting substances made up of five CFCs (CFC-12, CFC-11, CFC-113), three HCFCs (HCFC-22, HCFC-141b, HCFC-142b), two halons (Halon-1211, Halon-1301), CH_3CCl_3, CCl_4, CH_3Cl, methylene chloride (CH_2Cl_2), chloroform ($CHCl_3$), methyl bromide (CH_3Br) and HFC-134a~~and the~~ , and their associated photochemical reactions are included in the INCA chemical scheme to produce Cl radicals (Terrenoire et al., in preparation, 2019). In ~~the~~ LMDz-INCA simulations, the surface concentrations of these long-lived Cl source species are prescribed according to ~~the~~ historical datasets prepared by Meinshausen et al. (2017). The final Cl field will be referred to hereinafter as the LMDz-INCA field.

Figure 1 shows the key features of the resulting atomic Cl climatological fields averaged ~~for~~ over the 2003-2009 period. We use a climatological field for Cl due to a lack of simulations for more recent years and to avoid uncertainties in simulated ~~interannual variabilities and trends in Cl concentrations. However~~ inter-annual variabilities and Cl concentration trends. Nevertheless, a sensitivity test was performed to assess whether the recent decline of Cl could have a substantial impact on ^{13}~~C~~CH_4:^{12}~~C ratio values. This is~~ CH_4 ratio values, as discussed further in Section 3.5.2. The global mean volume-weighted stratospheric Cl atom concentration is about 3.25 $\times$ 10^5 ~~atoms.cm^{-3}~~atoms cm^{-3}. Acid displacement from sea salt aerosol (main source of tropospheric Cl) was not implemented in the model because the study mainly focuses on stratospheric Cl. Therefore, the tropospheric background mean (240 ~~atoms.cm^{-3}~~atoms cm^{-3}) is smaller than the results of studies focus-

ing specifically on troposphere such as Hossaini et al. (2016) ~~which presents a background of~~ or Wang et al. (2019), whose background values are 1300 ~~atoms.cm^{-3} or Wang et al. (2019)with a background of~~ and 620 ~~atoms.cm^{-3}. Nevertheless, Hossaini et al. (2016)~~ atoms cm^{-3}, respectively. Therefore, our values in the troposphere may be underestimated. Cl concentrations well above 1000 ~~atoms.cm^{-3}~~ atoms cm^{-3} at the surface ~~might~~ from Hossaini et al. (2016) might nevertheless be overestimated according to Gromov et al. (2018). Figure 1b shows the time evolution of ~~the~~ atomic Cl concentrations over ~~the~~ a climatological year. The processes by which increased ~~photolysis within polar vortices~~ illumination in polar regions leads to more active Cl are ~~well-represented and should be a key parameter of the seasonal variability of simulated stratospheric methane in those regions. Lower latitude regions do not present such large fluctuations.~~ well represented. Chlorine reservoirs (HCl and $ClONO_2$) are converted to active chlorine on polar stratospheric clouds (PSCs) and/or cold binary sulphate through heterogeneous reactions (Nakajima et al., 2016; Solomon, 1999) :

$$N_2O_5 + HCl\,(s,l) \rightarrow Cl_2\,(g) + HNO_3 \quad \text{(R5)}$$

$$N_2O_5 + H_2O\,(s,l) \rightarrow HOCl + HNO_3 \quad \text{(R6)}$$

When solar illumination is available, Cl_2, $HOCl$, and $ClNO_2$ are photolyzed to produce atomic chlorine through the following reactions:

$$Cl + h\nu \rightarrow Cl + Cl \quad \text{(R7)}$$

$$HOCl + h\nu \rightarrow Cl + OH \quad \text{(R8)}$$

$$ClNO_2 + h\nu \rightarrow Cl + NO_2 \quad \text{(R9)}$$

2.4 Total CH_4 surface fluxes

~~The surface fluxes prescribed to simulate total methane mixing ratios are the ones suggested by the Global Carbon Project (GCP) as a priori~~ We adopt the CH_4 emissions suggested to be used as prior emissions for inversions performed ~~for~~ as part of the Global Methane Budget (Saunois et al., 2019). Anthropogenic (including biofuels) and fire emissions for the 2000-2017 period are ~~taken from bottom-up estimates provided by~~ based from the EDGARv432 ~~(http://edgar.jrc.ec.europa.eu/overview.php?v=432SECU~~ (http://edgar.jrc.ec.europa.eu/overview .php?v=432SECURE=123) (Janssens-Maenhout et al., 2017) and the GFED4s databases (van der Werf et al., 2017), respectively. Statistics from British Petroleum (BP) and the Food and Agriculture Organization of the United Nations (FAO) have been used to extend the EDGARv432 database, ending 2012, until 2017. The natural sources emissions are based on averaged literature values : Poulter et al. (2017) for ~~the~~ wetlands, Ridgwell et al. (1999) for ~~the~~ soil sink, Kirschke et al. (2013) for ~~the~~ termites, Lambert and Schmidt (1993) for ~~the~~ ocean and Etiope (2015) for geological sources. ~~All the sectors and their emission intensities averaged over the 2006-2018~~ Averaged emissions fluxes over the 2000-2018 period are listed in Table ~~2. The emissionsfor~~ 2 for both anthropogenic and natural emissions. Emissions for the year 2018 have been set equal to 2017. ~~Figure S2 shows the evolution over time of methane emissions for each sector.~~ CH_4 emissions from natural sources are kept constant over the ~~period of time considered~~ time-window, while anthropogenic emissions linearly increase ~~.~~

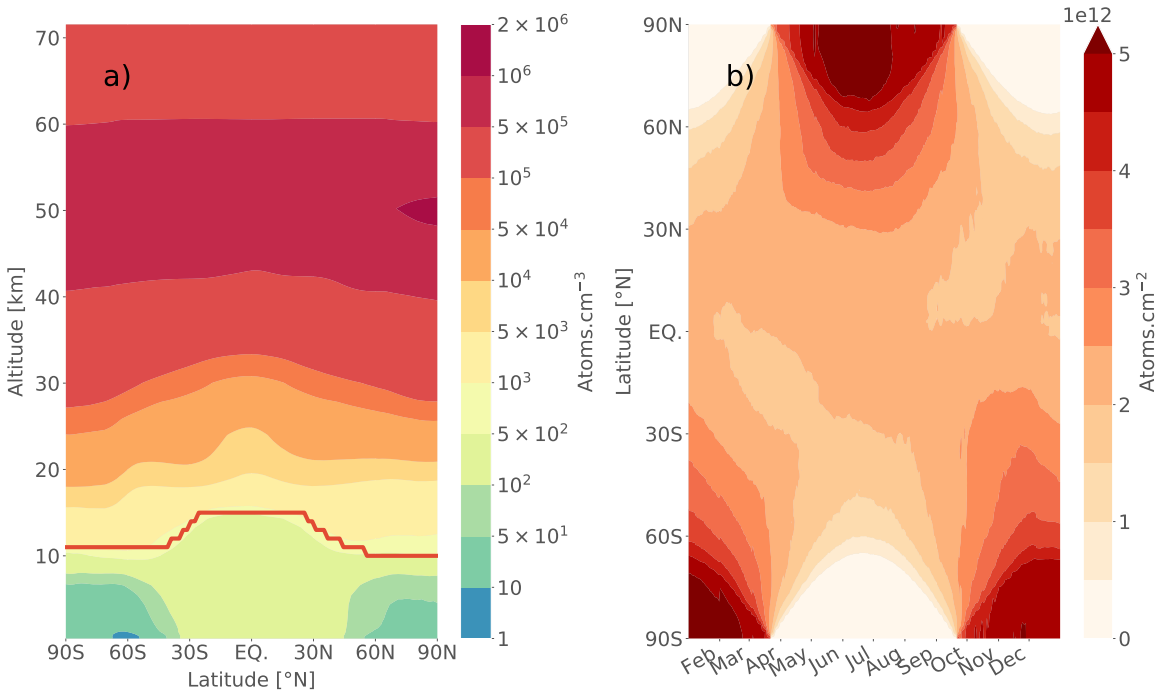

Figure 1. 3-D LMDZ-INCA climatological field of Cl for the 2003-2009 period. a) Meridional cross-section of Cl concentrations in $\mathrm{atoms\,cm^{-3}}$. The red line represents the mean tropopause level. b) Time evolution of meridional Cl total column in $\mathrm{atoms\,cm^{2}}$. The total column have been computed using volume-weighted integration.

~~The anthropogenic~~ (Figure S2). Anthropogenic sources account for 61 ± 2 % (1σ for ~~interannual~~ inter-annual variability) and ~~the~~ natural sources for 39 ± 2 % of the total ~~global budget~~emission.

2.5 Sources δ^{13}C isotopic signatures

The ^{13}~~C~~CH_4:^{12}~~C~~ CH_4 ratio is reported through the δ^{13}~~C~~ C-CH_4 value defined by :

$$\delta^{13}C_{sample}C-CH_4 = \frac{R}{R_{std}}\frac{R}{R_{\mathrm{std}}} - 1 \quad (2)$$

R is the ^{13}~~C~~CH_4:^{12}~~C~~ CH_4 ratio of the sample and ~~R_{std}~~ R_{std} is the standard ^{13}~~C~~CH_4:^{12}~~C~~ CH_4 ratio taken as a reference scale. In this paper, the signature is computed ~~according~~ relatively to the Vienna - Pee Dee Belemnite (V-PDB) standard reference ratio ($R_{V-PDB} = 0.0112372\ \mathrm{mol.mol^{-1}}$) (Craig, 1957). The two species $^{12}CH_4$ and $^{13}CH_4$ are simulated separately in LMDz. ~~Each individual source is assigned an isotopic signature~~ An isotopic signature is assigned to each individual source and the amount of $^{12}CH_4$ and $^{13}CH_4$ emitted from this source can be easily inferred from its signature and the ~~intensity of the total methane emission~~ flux of total CH_4 emissions ($^{12}CH_4$ + $^{13}CH_4$) from this source using the equations below :

$$F_{13} = (1+\delta^{13}C)R_{std\text{std}} \times \frac{M_{13}}{M_{12}} \times F_{12} \quad (3)$$

$$\frac{F_{12}}{M_{12}} + \frac{F_{13}}{M_{13}} = \frac{F_{TOT}}{M_{TOT}} \frac{F_{\text{TOT}}}{M_{\text{TOT}}} \quad (4)$$

~~F_{TOT}~~ F_{TOT}, F_{13} and F_{12}, denote the total CH_4, $^{13}CH_4$ and $^{12}CH_4$ ~~mass fluxes~~ fluxes in mass, respectively. ~~M_{TOT}~~ M_{TOT}, M_{13} and M_{12} ~~correspond to~~ are their molar masses. ~~Unlike the other sinks, we consider the soil sink as a negative source~~ The soil sink is converted into a prescribed field (solely active at the surface~~. Therefore we define an effective δ^{13}C-CH_4 signature ($\delta^{13}C_{eff}$) based on the KIE of the soil sink and~~) and incorporated into the model as the other sinks. More details are provided in the ~~mean ^{13}C:^{12}C ratio at surface :~~

$$\delta^{13}C_{eff} = \frac{1+\delta^{13}C_{amb}}{KIE_{soil}} - 1$$

~~$\delta^{13}C_{amb}$ denotes the atmospheric isotopic signal near the surface. A mean value of − 47.2 ‰ set constant over time is prescribed. This value is in good agreement with the observed records (see Sect. 3.5). A KIE_{soil}~~ supporting information. A KIE_{soil} of 1.020 (Snover and Quay, 2000; Reeburgh et al., 1997; Tyler et al., 1994; King et al., 1989) ~~was chosen. It leads to a $\delta^{13}C_{eff}$ of -65,9 . The signatures of each sector~~ is prescribed.

Isotope source signatures are based on literature average values and summarized in Table 2. We use region-specific signatures over ~~the~~ 11 regions ~~of~~ derived from the TransCom project (see Figure ~~S4~~S6) for wetlands, gas and biofuels-biomass ~~sectors that exhibit a strong regional variability of signatures. The signature is set globally uniform for the other sectors~~categories that exhibit strong regional variabilities in signatures. A global signature value is prescribed to the other categories. All signatures are set constant over time. More information about the regional isotopic ~~signature~~ signatures and the references are provided in the supporting information (Text S1). ~~The isotopic signatures of wetland emissions are inferred~~ Wetlands isotopic signatures were taken from multiple regional studies around the world and aggregated into a 11-regions map, in order to be consistent with the other ~~sectors. Initially, this wetlands~~ categories. This wetland isotopic signature map was used to run the first simulations but ~~we realized~~ it appears that the flux- and area-weighted signature ~~can appear~~ was high compared to other papers (Feinberg et al., 2018; Ganesan et al., 2018) ~~which~~ that studied isotopic signature values at a finer resolution. Overestimated isotopic signatures in boreal regions may be the cause of this difference. Therefore, the isotopic signature map from Ganesan et al. (2018) for wetland emissions has also been used to assess the impact of a lower global isotopic signature. In Sect. 3.5.1, it is briefly shown that taking this lower signature does not affect the conclusions of ~~our paper~~this study.

Table 2. ~~Intensities~~ Annual flux and mean (flux- and area-weighted) isotopic signatures of ~~methane~~ CH_4 sources averaged over 2000-2018 for natural and anthropogenic categories. ~~The~~ Min and max over the time-window are displayed in brackets for anthropogenic sources that exhibits inter-annual variability. The isotopic source signatures with a * symbol are prescribed with a regional variability. The value given here is the mean over the 11 regions. Min and max are displayed in parentheses. Soil sink is included in order to compare its intensity to other categories.

Natural sources/sinks	~~**Intensity**~~ **Annual flux** (Tg/yr)	**δ^{13}C signature** ~~δ^{13}C~~ (‰)	**Anthropogenic sources**	**Annual flux** ~~**Intensity**~~ (Tg/yr)	**δ^{13}C signature** ~~δ^{13}C~~ (‰)
Wetlands	180.2	-58.6 (-65.0/-50.0)*	Livestock	112.3 [102.2 – 120.7]	-61
Termites	8.7	-63	Rice cultivation	36.0 [32.5 - 38.8]	-63
Ocean	14.4	-42	Oil, Gas, Industry	71.2 [61.2 – 78.8]	-39.7 (-54.7/-40.7)*
Geological (onshore)	15.0	-50	Biofuels - Biomass	27.6 [23.6 – 35.5]	-25.8 (-24.9/-20.9)*
Soil	-37.9	~~-65.9~~ KIE_{soil}=1.020	Waste	66.1 [59.4 – 72.9]	-49.7
			Coal	32.5 [21.9 – 38.8]	-35
Total	526.5 [483.6 - 555.2]	-51.1 [-51.6 – -50.5]			

2.6 Observations

2.6.1 AirCore ~~measurements~~profiles of CH_4

An original set of 115 total ~~methane~~ CH_4 vertical profiles retrieved above 11 different locations during the 2012-2018 period is used to compare the results of the simulations to observed values. A total of 80 profiles (NOAA GGGRN AirCore_v20181101 dataset) are provided by the NOAA-ESRL Aircraft Program (Karion et al., 2010) and an additional 35 by the French AirCore Program (Membrive et al., 2017). ~~Those~~ These vertical profiles have all been collected using ~~the~~ AirCore technique (Karion et al., 2010). This technique retrieves air samples ~~going~~ from the surface to approximately 30km. ~~The locations and the number of profiles associated are shown in Figure 2. This dataset has also been used in this study to analyze the seasonal vertical trend of CH_4 in both the troposphere and stratosphere and the model ability to reproduce the observations depending on the season. A summary of the information~~ Information about the provider, the location and the number of profiles retrieved ~~at this location~~ is given in Table ~~3. The CRDS analyzer~~ 3 and Fig. 2. The precision of the ~~measurements of the AirCore sample for~~ CRDS analyzer used for the measurements of AirCore samples from both NOAA and French AirCore Program is less than 2 ppb for CH_4, which is generally much smaller than the ~~model-observation mismatch.~~ model-obs mismatch. This dataset also provides information regarding seasonal variations in the CH_4 profile in both the troposphere and stratosphere.

2.6.2 Balloon vertical profiles of δ^{13}~~C~~C-CH_4

We use air samples from stratospheric balloon flights ~~from~~ analyzed in Röckmann et al. (2011) to compare ~~the~~ simulated δ^{13}C-CH_4 to observations ~~. The information is summarized in Table 4.~~ (see Table 4). The samples were retrieved at four different locations ~~going~~ from subtropical to high latitudes, above an altitude of 10 km and up to 35 km. ~~We assume that~~

Table 3. Providers, locations and number of vertical profiles of ~~total methane~~ CH_4 retrieved using AirCore technique between 2012 and 2018. The longitude and latitude given here are means over the AirCore descent profile.

Provider	Location	Number of profiles	Longitude	Latitude
NOAA-ESRL Aircraft Program	Edwards AFB/Dryden, USA	6	-117	34
	Boulder, CO, USA	33	-103	40
	Lamont, OK, USA	30	-97	36
	Park Falls, WI, USA	4	-90	46
	Sodankyla, Finland	6	26	67
	Lauder, NZ	1	169	-45
French AirCore Program	Alice Springs, Australia	3	133	-23
	Aire-sur-l'Adour, France	9	1	43
	Trainou, France	17	2	48
	Timmins, Ontario, Canada	4	-83	48
	Esrange, Northern Sweden	2	21	67

~~δ^{13}C-CH_4 vertical profiles do not exhibit a strong inter-annual variability and therefore we can compare our simulations and the observations retrieved before 2000.~~ Uncertainties are generally below 0.2 ‰.

2.6.3 Surface δ^{13}~~C~~ C-CH_4 observations

Multiple surface stations from the Global Greenhouse Gas Reference Network (GGGRN), part of NOAA-ESRL Global Monitoring Division (NOAA-ESRL GMD), are collecting air samples on an approximately weekly basis. Those air samples are analyzed by the Institute of Arctic and Alpine Research (INSTAAR) to provide ~~isotopic measurements of~~ CH_4 ~~. 18 stations that recorded enough~~ isotope ratio measurements. 11 MBL sites (i.e. samples from the site are predominantly of well-mixed MBL air) that recorded δ^{13}C-CH_4 values during the 2000-2018 period ~~to estimate a~~ were selected. Averaging those values provides a global δ^{13}C-CH_4 ~~range over this period and the negative trend that started around 2007 were selected~~mean time-series spanning the simulated time-window. Only monthly values were aggregated. The locations of the selected stations are given in Figure 2 (green circles). These observations will be referred to as NOAA-GGGRN surface observations.

2.7 Simulations performed

2.7.1 ~~Total methane simulations~~

~~To assess the impact of Cl in the stratosphere on total methane, we perform two simulations with TOT_CHL and without TOT_REFthe Cl sink implemented~~ We perform one reference simulation (REF) and a set of 7 sensitivity tests (Table 5) with different Cl concentrations in the troposphere and in the stratosphere. We simulate ~~total methane~~ in parallel $^{12}CH_4$ and $^{13}CH_4$

Table 4. ~~Overview of balloon~~ Balloon flights and number of samples analyzed for δ^{13}~~C~~C-CH_4. Each flight is given a flight ID as STA-JJ-MM, where STA is the 3-letter-code for the balloon launch station, JJ the year and MM the month of sampling. This Table is adapted from Röckmann et al. (2011). [1] HYD: Hyderabad, India (17.5 °N, 78.60 °E); [2] KIR: Kiruna, Sweden (67.9 °N, 21.10 °E); [3] ASA: Aire sur l'Adour, France (43.70 °N, 0.30 °E); [4] GAP: Gap, France (44.44 °N, 6.14 °E);

Flight ID	Flight Date	Location	^{13}C	Characteristics
Flights operated by MPI für Sonnensystemforschung				
HYD-87-03	03/26/87	HYD[1]	5	Subtropical
KIR-92-01	01/18/92	KIR[2]	13	Artic weak vortex, final warming series
KIR-92-02	02/06/92	KIR[2]	10	Final warming series
KIR-92-03	03/20/92	KIR[2]	10	Final warming series
ASA-93-09	09/30/93	ASA[3]	15	Mid-latitudinal background
KIR-95-03	03/07/95	KIR[2]	15	Artic with mid-latitudinal characteristics
HYD-99-04	04/29/99	HYD[1]	10	Subtropical
GAP-99-06	06/23/99	GAP[4]	15	Mid-latitudinal summer
Flights operated by Institut für Meteorologie und Geophysik, Universität Frankfurt				
KIR-00-01	01/03/00	KIR[2]	13	Artic strong vortex
ASA-01-10	10/11/01	ASA[3]	13	Mid-latitudinal background
ASA-02-09	09/15/02	ASA[3]	13	Mid-latitudinal background
KIR-03-03	03/06/03	KIR[2]	13	Arctic vortex, mesospheric enclosure
KIR-03-03	06/09/03	KIR[2]	13	Artic summer

mixing ratios for the ~~2006-2018~~ 2000-2018 period starting from the same initial conditions, and ~~use the varying GCP~~ using monthly varying CH_4 emissions (see Sect. 2.5). CH_4 is defined as the sum of the two tracers.

The initial conditions for the REF simulation have been obtained using ~~optimized fluxes from results of inversions performed by Locatelli et al. (2015a). The simulated vertical profiles of total methane are compared to AirCore measurements in Sect. 3.2.~~

2.7.1 ~~Methane isotope simulations~~

~~We simulated in parallel $^{12}CH_4$ and $^{13}CH_4$ concentrations, so that the sum of $^{12}CH_4$ and $^{13}CH_4$ is set equal to total CH_4. Since δ^{13}C-CH_4 simulated values need a larger time to adjust (Tans, 1997), we first performed a 19-year~~ a 30-year spin-up using ~~constant emissions of~~ emissions and meteorology for the year 2000 including all chemical sinks ~~and starting in 2000~~ in order to obtain a good spatial and vertical distribution of CH_4 mixing ratios and δ^{13}C-CH_4 values. ~~Then we adjusted the simulated isotopic signal to the~~ For the spin-up run, CH_4 mixing ratios from Locatelli et al. (2015b) inferred using an inversion system were used as initial conditions for total CH_4. Additionally, δ^{13}C-CH_4 values inferred from globally averaged observations were prescribed at the surface and the Rayleigh fractionation equation was applied to infer a realistic δ^{13}C-CH_4 vertical profile.

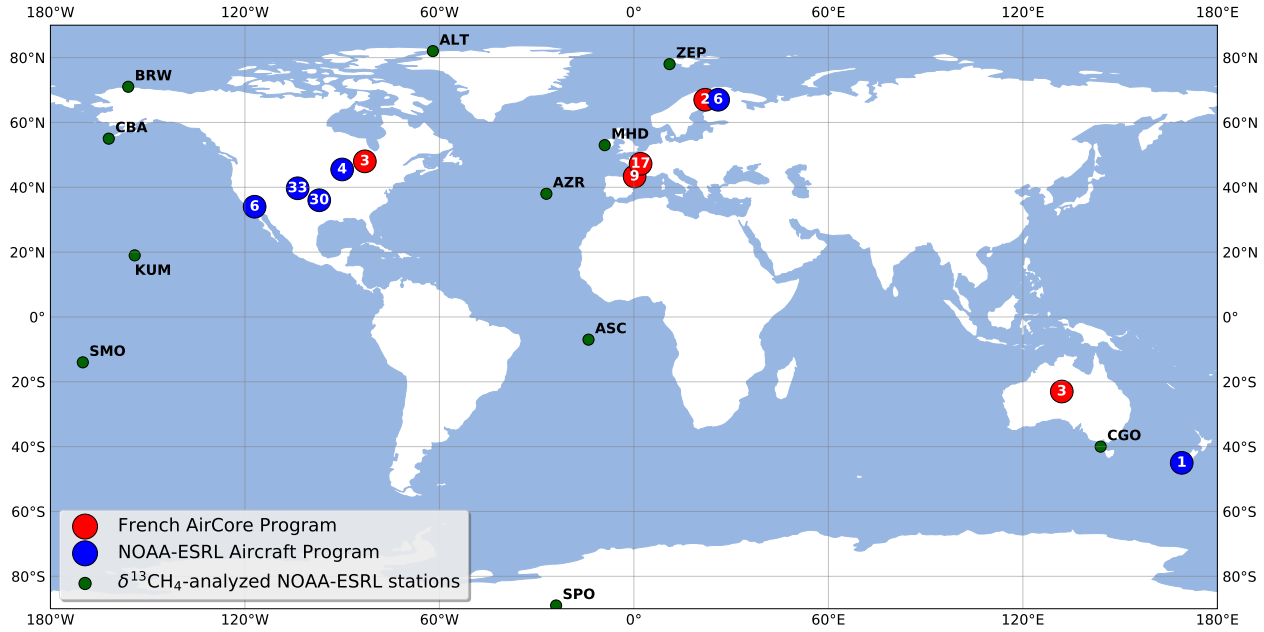

Figure 2. Locations of AirCore vertical profiles ~~retrievals~~ and NOAA-GGGRN ~~stations~~surface sites. The number inside each AirCore location markers indicates the number of different profiles retrieved at each location.

There is a 0.04 ‰ difference between the observed δ^{13}C-CH_4 global mean at the surface based on available NOAA-GGGRN δ^{13}C-CH_4 surface observations~~(see Sect. 2.6.3) in order to obtain satisfying initial conditions~~) in 2000 and the output from the spin-up. No adjustment is performed due to non-linearity of transport, mixing and fractionating sink processes. From these initial conditions, we run an ensemble of scenarios ~~for 19 years (~~spanning 2000-2018 ~~) using constant sources of year 2000~~using transient emissions, and varying the ~~chemical sink of methane through Cl. The characteristics of each sensitivity test~~ Cl sink of CH_4. Sensitivity test characteristics are summarized in Table 5.

The LMDz-INCA Cl field used in the S1 simulation exhibits a global tropospheric mean value of 240 $\mathrm{atoms\,cm^{-3}}$ and a MBL mean value of 130 $\mathrm{atoms\,cm^{-3}}$. In the S2 scenario, the tropospheric Cl is removed. In S3, the stratospheric Cl is removed. In S4, the tropospheric global mean of Cl concentrations is scaled to 620 $\mathrm{atoms\,cm^{-3}}$, as reported by Wang et al. (2019). In S5, the tropospheric mean is scaled to the values of Wang et al. (2019), i.e. 620 $\mathrm{atoms\,cm^{-3}}$ in the troposphere and 1200 $\mathrm{atoms\,cm^{-3}}$ in the MBL. In S6, the Cl concentrations are decreasing by 5% per decade from 2000 to 2018. Finally, S7 is the same as the latter but with the tropospheric concentrations from Wang et al. (2019).

3 Results

3.1 Impact of Cl sink on ~~total methane~~ CH_4 mixing ratios

Table 5. Nomenclature and characteristics of simulations. See Sect. 3.1 for more information about the sensitivity tests.

Simulation name	Traced species	Cl-CH_4 Reaction	Simulation period	Tropospheric chlorine	MBL chlorine	Stratospheric chlorine	Decreasing chlorine
REF	$^{12}CH_4$ - $^{13}CH_4$	~~YES~~ NO	2000-2018	~~240~~ NO	~~130~~ NO	~~YES~~ NO	~~NO~~ NO
Sensitivity tests							
S1	$^{12}CH_4$ - $^{13}CH_4$	~~NO~~ YES	2000-2018	240 cm^{-3}	130 cm^{-3}	YES	NO
~~S5~~ S2	$^{12}CH_4$ - $^{13}CH_4$	YES	2000-2018	NO	NO	YES	NO
~~S6~~ S3	$^{12}CH_4$ - $^{13}CH_4$	YES	2000-2018	240 cm^{-3}	130 cm^{-3}	NO	NO
~~S7~~ S4	$^{12}CH_4$ - $^{13}CH_4$	YES	2000-2018	620 cm^{-3}	335 cm^{-3}	YES	NO
~~S8~~ S5	$^{12}CH_4$ - $^{13}CH_4$	YES	2000-2018	620 cm^{-3}	1200 cm^{-3}	YES	NO
~~S9~~ S6	$^{12}CH_4$ - $^{13}CH_4$	YES	2000-2018	240 cm^{-3}	130 cm^{-3}	YES	5% ~~/~~per decade
~~S10~~ S7	$^{12}CH_4$ - $^{13}CH_4$	YES	2000-2018	620 cm^{-3}	1200 cm^{-3}	YES	5% ~~/~~per decade

~~Nomenclature and characteristics of the simulations. See Sect. 3.5 for more information about the sensitivity tests.~~

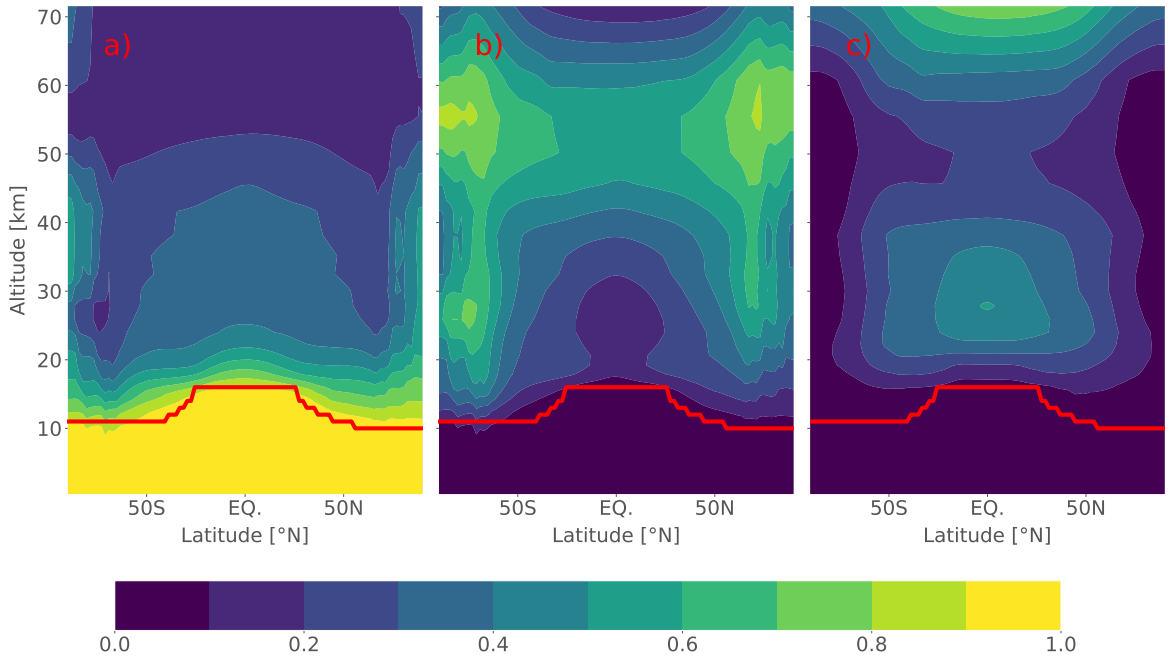

Figure 3. Global distribution of ~~the~~ relative contribution ~~of~~ from each ~~methane~~ CH_4 sink to the total chemical sink. The ~~green~~ red line indicates the mean tropopause level. a) OH contribution to the sink. b) Cl contribution. c) $O(^1D)$ contribution.

~~We analyze the simulated methane mixing ratios of TOT_REF and TOT_CHL during the 2006-2018 period.~~ The total stratospheric ~~sink for methane~~ CH_4 sink is found to be ~~equal to~~ 24.68 ± 0.73 (1σ for ~~interannual~~ inter-annual variability) Tg/yr on

average over ~~the 2006-2018 period of simulation~~ 2000-2018 (∼ 5.3 % of total atmospheric sink) in REF. The simulations yield a stratospheric Cl sink of 7.16 ± 0.27 Tg/yr, thus ~~accounting for~~ contributing about 29% ~~of~~ to the total stratospheric sink. This result is at the lower end of the range estimated ~~by former papers~~ previously for the period 2000-2009 ~~(Kirschke et al., 2013) Saunois et al. 2019~~(Kirschke et al., 2013; Saunois et al., 2019) : [16-84] Tg for total stratospheric loss with a Cl contribution between 20 and 35%.

Figure 3 shows the relative contribution of each sink to the total sink in ~~each latitude/altitude box of~~ the model. We use the lapse rate (2 K/km) definition from the World Meteorological Organization (WMO) to define the tropopause. Below the tropopause, OH is mostly responsible for the removal of ~~methane~~ CH_4 (97% of the chemical sink) as expected~~, but it contributes only for~~ . In the stratosphere, it accounts for only 45 % on average~~in the stratosphere :~~ , the rest of the ~~methane sink is~~ CH_4 sink being due to reactions with Cl and $O(^1D)$. We estimate that the Cl sink can reach 40-60 % of the total sink strength at high latitudes between 20 and 40 km of altitude and 60-80% above 40 km. Between 20 and 40 km altitude, the sink associated with $O(^1D)$ is responsible for half of the total sink in tropical regions due to ~~the~~ high O_3 photolysis rates ~~there~~ but only 30-40% at higher altitudes where enhanced Cl concentrations contribute 50-60% to the total chemical sink. Note that, as explained in Section 2.3, our Cl concentrations in the troposphere ~~are likely to be underestimated~~ and its relative overall contribution of 1.23 ± 0.02 Tg/yr ~~as well~~are likely to be underestimated.

The change in ~~methane~~ CH_4 mixing ratio due to the implementation of the Cl sink does not exceed 10 ppb in the troposphere (0,5 % of the tropospheric mixing ratio). However, it can lead to a reduction of up to 225 ppb between 50 and 60 km (∼ 50 % of the mixing ratio at this level) as well as 100 ppb above 20 km in the extratropics and 30 km in the tropics (∼ 8 %).

These results confirm that the ~~Cl sink in the stratosphere~~ stratospheric Cl sink accounts for a large ~~proportion~~ amount of the simulated ~~methane~~ CH_4 chemical sink in some regions of the atmosphere.

3.2 ~~Impact of Cl on methane total column~~

~~The impact of Cl on the~~ The inclusion of Cl influences the CH_4 seasonal cycle slightly at the surface but more significantly near the tropopause and above. In our model, at the surface, the seasonal cycle amplitude increases by 0.8 % - 0.9 % at global scale and by 0.8 % - 1.3 % in polar regions depending on the scenario, which is very low. Above 15 km, this increase can reach 12% at global scale and 21 % in polar regions. As expected, the most significant changes are seen above the tropopause where the Cl sink highly impacts total CH_4 removal.

3.2 Impact of Cl on CH_4 total column

Impact of Cl on dry-air column average ~~mole fraction of methane~~ mixing ratios of CH_4 (XCH_4) is also an important element to consider. This quantity is computed as the ratio of ~~methane~~ CH_4 column density to dry-air column density. The value is here determined using a dry-air weighted mass average of the mixing ratio. Dry-air column average ~~mole fraction~~ mixing ratio will be referred to hereinafter as the simple term 'column'. ~~Remotely sensed~~ Remotely-sensed total column retrievals are often used in inversions as additional constraints (or as an independent validation) and errors in the ~~total column modeling due to the~~ simulated total column due to a missing Cl sink could significantly influence the results of an inversion.

~~We assess that after a 12-year simulation from 2006 to 2018~~After a 19-year run spanning 2000-2018, the difference of ~~global mean~~ global-mean total columns between ~~TOT_REF and TOT_CHL is 18 ±~~ REF and S1 in 2018 is 21.9 ± 0.4 ppb (1σ for spatial and ~~time variability) for the year 2018~~ seasonal variability) which represents a ~~1~~1.2% difference. This difference tends to increase by about 2 ppb/yr over the 2000-2006 period, 1 ppb/yr over the ~~2012-2018 period and 1.5~~ 2006-2012 period and 0.5 ppb/yr over the ~~2006-2012 period. The difference~~ 2012-2018 period. This is due to an adjustment time and a difference of source ~~intensities between the two periods.~~ fluxes between the three periods. Greater discrepancies are observed over high-latitude regions where Cl concentrations are higher. Figure 4 shows ~~the total column regional variability~~ total column distribution averaged over the year 2018, and the differences between ~~TOT_REF and TOT_CHL. It also includes the~~ REF and S1 in total column and tropospheric and stratospheric partial columns ~~differences~~ (Fig. 4b, Fig. 4c and Fig. 4d). The difference in tropospheric columns ~~is as high as 10.6 ppb~~ between the two simulations ~~, but with only a very small geographical variability of the tropospheric column difference (of typically 0.1 ppb around 10.6 ppb ,~~ is as high as 13.9 ppb ± 0.2 ppb (see Figure 4c). ~~Most~~ However, most of the total column regional variability comes from the stratosphere. The stratospheric partial column difference ~~has a zonal distribution. It shows a variability of 7.7 ppb (1σ for spatial variability) and the~~ shows a clear zonal distribution, with minimum values in the tropics (around 35 ppb) and maximum values (up to ~~60 ppb) are found~~ 65 ppb) in high-latitude regions. ~~The extreme~~

Extreme values found over Greenland and Antarctica are strongly correlated ~~to the~~ with orography. The ratio of the ~~mass in the stratosphere to that in the total column~~masses (stratosphere partial column to total column) is larger in regions where the surface is higher ~~and, in~~ in altitude. In addition, the Cl sink has larger impact in the stratosphere. Therefore, the total ~~methane~~ CH_4 column difference shows greater values ~~(difference of more than 5 ppb)~~ over those high ~~regions~~places. However, they do not strongly influence the ~~mean column averaged over the globe~~ global-mean column value since the total dry-air mass above is smaller.

~~The total column difference (Fig. 4b) shows difference reaching 1% to 2% of the methane column after a 12-year simulation. This result may change depending on the averaging kernel used for comparison to vertical profiles retrieved by remote sensing techniques.~~

3.3 ~~Total methane~~ CH_4 vertical profiles

The set of total ~~methane~~ CH_4 vertical profiles retrieved using ~~the~~ AirCore technique is used to assess ~~how much the implementation of the Cl sink in the model improves simulations~~potential improvement of the model due to Cl sink implementation. Since the ~~methane~~ CH_4 mixing ratio reduction due to the Cl sink is proportional to the amount of ~~methane~~ CH_4 present in the atmosphere, ~~the~~ a reduction ratio is more relevant to assess the impact of Cl, while the reduction itself is better to quantify ~~the~~ model ability to match ~~the observations. We compute the reduction ratio using the following equation :~~

$$r = \frac{(m_{REF} - m_{CHL})}{(m_{REF} - o)} \times 100$$

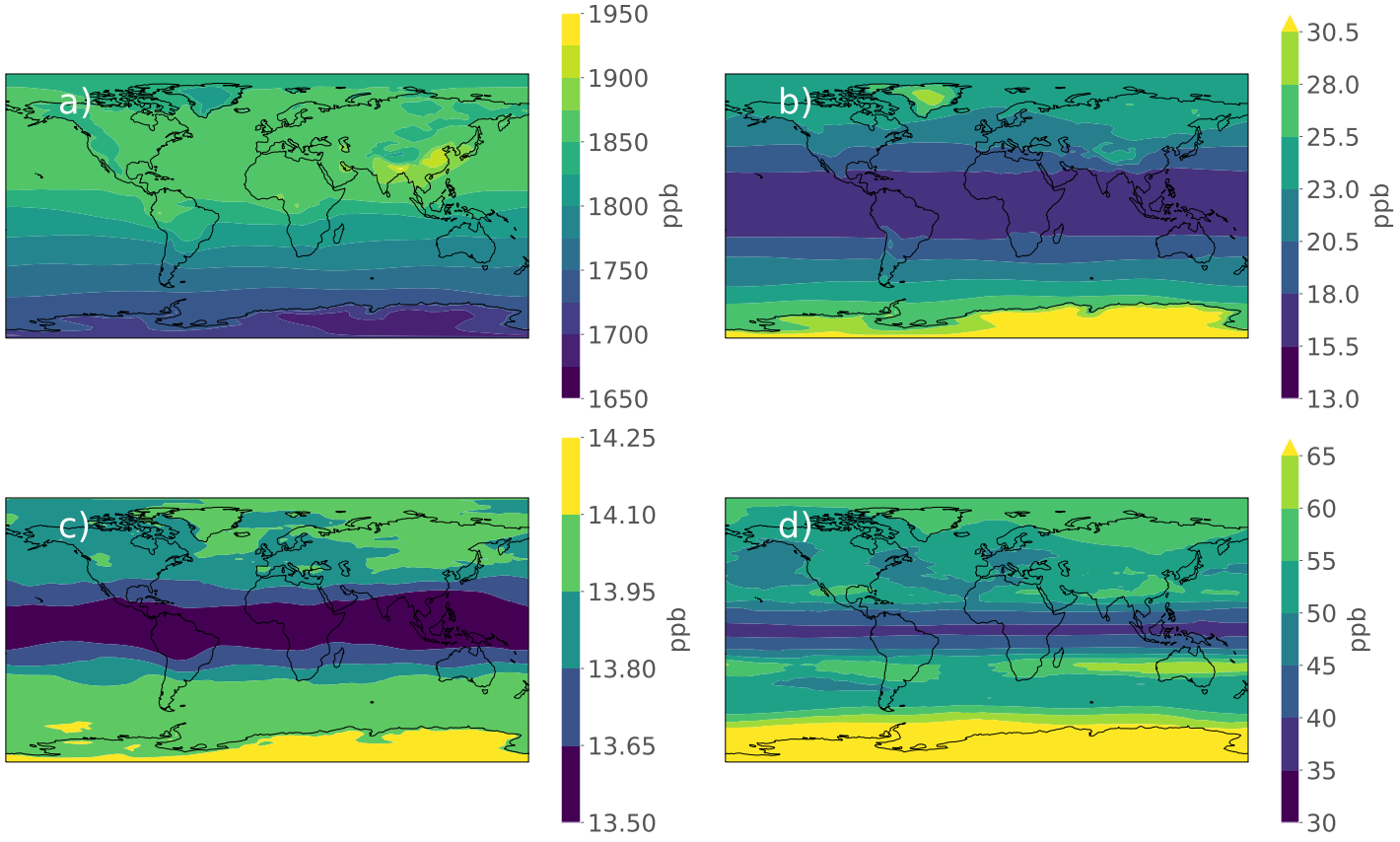

Figure 4. ~~Dry-air~~ Total column average ~~mole fraction of methane (a) and differences~~ mixing ratio of ~~methane total and partial columns between simulations (TOT_REF - TOT_CHL) averaged~~ CH_4 from S1 an average over 2018 ~~in ppb ;~~ (a)~~Dry-air column average mole fraction of methane TOT_CHL~~. Differences in total column (b)~~Dry-air column average mole fraction difference. ,~~ and tropospheric (c) ~~Tropospheric methane partial column difference.~~ and stratospheric (d) ~~Stratospheric methane~~ partial ~~column difference.~~columns between REF and S1 (as REF minus S1) an average over 2018.

~~r denotes the reduction~~ observations. Reduction ratio (or relative difference) ~~, m_{CHL}~~ r is defined by :

$$r = \frac{(m_{\mathrm{REF}} - m_{\mathrm{CHL}})}{(m_{\mathrm{REF}} - o)} \times 100 \tag{5}$$

m_{CHL} is the simulated value from ~~the TOT_CHL simulation, m_{REF}~~ S1, m_{REF} is the simulated value from ~~the TOT_REF simulation~~ REF and o is the observed value. The ~~smaller~~ closer the value of r is to zero, the better ~~is~~ the match between model results and observations.

We compute the difference between simulated and observed profiles after the simulated values have been linearly interpolated on the associated AirCore profile pressure axis. Points outside the data range ~~are~~ were extrapolated using the inferred

interpolation function. ~~The model-observation~~ model-obs discrepancy distributions are shifted to ~~the left towards~~ smaller values (reduction ratio smaller than 100 %) when including the Cl sink for all seasons in both the troposphere and stratosphere (Fig. 5). This illustrates ~~the improvement of the model~~ some modelling improvement when including Cl. We find that the implementation of ~~the~~ Cl sink reduces the difference between simulated and observed vertical profiles on average by ~~26.7~~ 31.7 ± ~~9.73~~ 13.2 % (1σ for intra-profile variability) in the stratosphere over the entire dataset and by ~~38.3~~ 59.3 ± ~~13.8~~ 24.8 % in the troposphere. This ratio represents a CH_4 reduction of about ~~24~~ 27 ppb in the stratosphere and ~~8.1~~ 9 ppb in the troposphere. ~~However, even including~~ Although the Cl sink ~~, the simulations shows~~ is included, simulations show significant remaining discrepancies in the troposphere compared to AirCore CH_4 observations (∼20 ppb, ~~1,1~~1.1% of the tropospheric mixing ratio) and in the stratosphere (∼85 ppb, 5.5% of the stratospheric mass-weighted mean mixing ratio).

The reason of this systematic error in the troposphere ~~might be due to the~~ is probably due to an overestimation of the emission scenario ~~from GCP which reflects the~~ used here, which reflects state of the art ~~of~~ bottom-up emission scenarios but is not optimized against atmospheric observations and not in adequate balance relative to the chemical sinks in ~~the~~ our model. Since 1) the errors are much larger in the stratosphere than in the troposphere and 2) the correction of the tropospheric bias would only (very likely) slightly shift the stratospheric values to smaller values, ~~not correcting for~~ this systematic error will not affect the conclusions in this work. Performing similar comparison using optimized fluxes based on inversions including the Cl sink would help to overcome this issue. However, the main objective of our study is to evaluate the impact of ~~the~~ Cl sink and not ~~really to~~ to perfectly fit to the observations. Further work will be dedicated to better match the observations ~~based on the results of atmospheric inversions from Saunois et al. (2019) and new ones using isotopic constraint~~using both total CH_4 and isotopic data. The underestimated Cl ~~concentration~~ concentrations in the MBL and more generally in the troposphere could also contribute to the bias simulated in the lower troposphere. Improving our estimates of Cl concentrations in the troposphere may help ~~reducing~~ reduce this tropospheric bias, which spreads upward into the stratosphere and is amplified by the discrepancies between observed and simulated vertical gradients.

Figure 5 shows the seasonal distribution of the differences (and reduction ratio) between ~~the~~ simulated and observed ~~by AirCore methane~~ CH_4 mixing ratio for the ~~tropospheric and stratospheric layers~~ troposphere and stratosphere with and without the Cl sink. The AirCore datasets provide multiple profiles for each season. Seasons are referred hereafter as North Hemispheric seasons, i.e. winter meaning boreal winter. Note that an AirCore profile retrieved above South Hemisphere locations is included in the list associated to its true season. For instance, an AirCore dataset retrieved during January in the South Hemisphere is added to the summer list. ~~The displayed value in each frame is the mean value of these differences over the considered region, namely~~ Then for each profile, mean differences for a specific layer of the atmosphere (troposphere or stratosphere) were calculated, and then displayed in the corresponding frame of Fig. 5 . The reduction ratio (third ~~line and sixth line~~and sixth row) ranges from ~~32~~ 45 % (spring) to ~~43~~71% (autumn) in the troposphere and from ~~23~~26% (spring) to ~~33~~42% (winter) in the stratosphere. Therefore, we ~~have~~ note larger reduction ratios in the troposphere than in the stratosphere, regardless of the season. The reduction is therefore greater in the troposphere relative to the stratosphere. However, this reduction ratio converted in a difference of mixing ratio is in a range of ~~6.69~~ 7 (autumn) - ~~10.50~~ 13 (spring) ppb in the troposphere and ~~19.26~~ 23 (winter) - ~~28.04~~ 32 (summer) ppb in the stratosphere. ~~The~~ Mixing ratio reduction is thus ~~much lower~~ greater (more than 10 ppb) in the

troposphere stratosphere than in the stratosphere. Nevertheless, the reduction in each region troposphere. Also, this analysis reveals a dependency on the season for each layer of the atmosphereis dependent on the season. Moreover, spring . Spring always exhibits the largest discrepancies after the Cl sink has been when Cl sink is implemented. Latitudinal dependence dependencies have not been analyzed since the numbers of AirCore profiles retrieved in high-latitudes regions is very low (see Figure 2).

Figure 6 displays the comparison between AirCore observations and associated simulated profiles (with the Cl sinkimplementedCl sink) linearly interpolated on a regular altitude axis following the same method as before. Above the tropopause between 15-25 km, the model-obs difference can exceed 150 ppb on average during spring and summer even with the Cl implementedCl sink. All the profiles and their associated simulated profiles are plotted in Figure S3S5. A closer analysis of individual profiles shows that more small-scale variations occur very localized mixing ratio spikes occur more often during spring and summer than during other seasons, especially around the tropopause. Additionally, inversions of concentrations mixing ratios can occur above the tropopause. Those may After analyzing outputs from the Monitoring Atmospheric Composition and Climate (MACC) project (Marécal et al., 2015), those are likely to be induced by small scale filaments of methane either high or low CH_4 coming from polar regions, that cannot be adequately reproduced by our low-resolution modelandseasonal averaging.

The profiles of vertical gradient are Vertical gradients are also plotted in Figure 6c. The values Data at the top of the profile (between 25 and 30 km) have been removeddiscarded from the analysis. Indeed, those values measurements cannot be easily interpreted due to the AirCore sampling methodology. We see that the high uncertainties at the uppermost portions of the AirCore sample. The simulated vertical gradient turns positive higher in altitude in comparison with the observations ($\sim$ 16-18 km for simulated gradients against 13-16 km for observed gradients), except for the simulated Simulated gradients in the DJF period , which are very close to observed gradients are closer to observations until 20 km, although very small differences compared to the others seasons can be noticed. This altitude difference leads to a positive difference between the observed and the simulated gradient. The simulated gradient tends to readjust re-adjust about 3-4 km higher in altitude (null difference) and then the gradient difference seem to turn turns negative above 20 km, meaning the simulated gradients might be overestimated at this level (see also Fig. 6a). Patra et al. (2011) and Thompson et al. (2014) pointed out that the LMDz version with 19 levels exhibited a too fast Stratosphere-Troposphere Exchange (STE) and a wrong tropopause height incorrect tropopause heights compared to other CTMs. (Locatelli et al., 2015a) Locatelli et al. (2015a) showed that increasing the number of levels from 19 to 39 levels acted to improve the flaw of LMDz regarding STE and tropopause height. However, the analysis of this large dataset of vertical profiles retrieved during different seasons suggests that STE errors are still therestill exist in the 39 level LMDz model. Furthermore, the discrepancies between simulated and observed mixing ratios at an altitude of 20 km can exceed 200 ppb, likely due to an underestimation of the Brewer-Dobson circulation intensity that transport the methane upward transports CH_4 into the upper stratosphere. The overestimation of the vertical gradient above 20 km also supports this hypothesis. Switching to isentropic coordinates as suggested by Patra et al. (2011) is more likely to reduce this error than increasing the number of vertical levels.

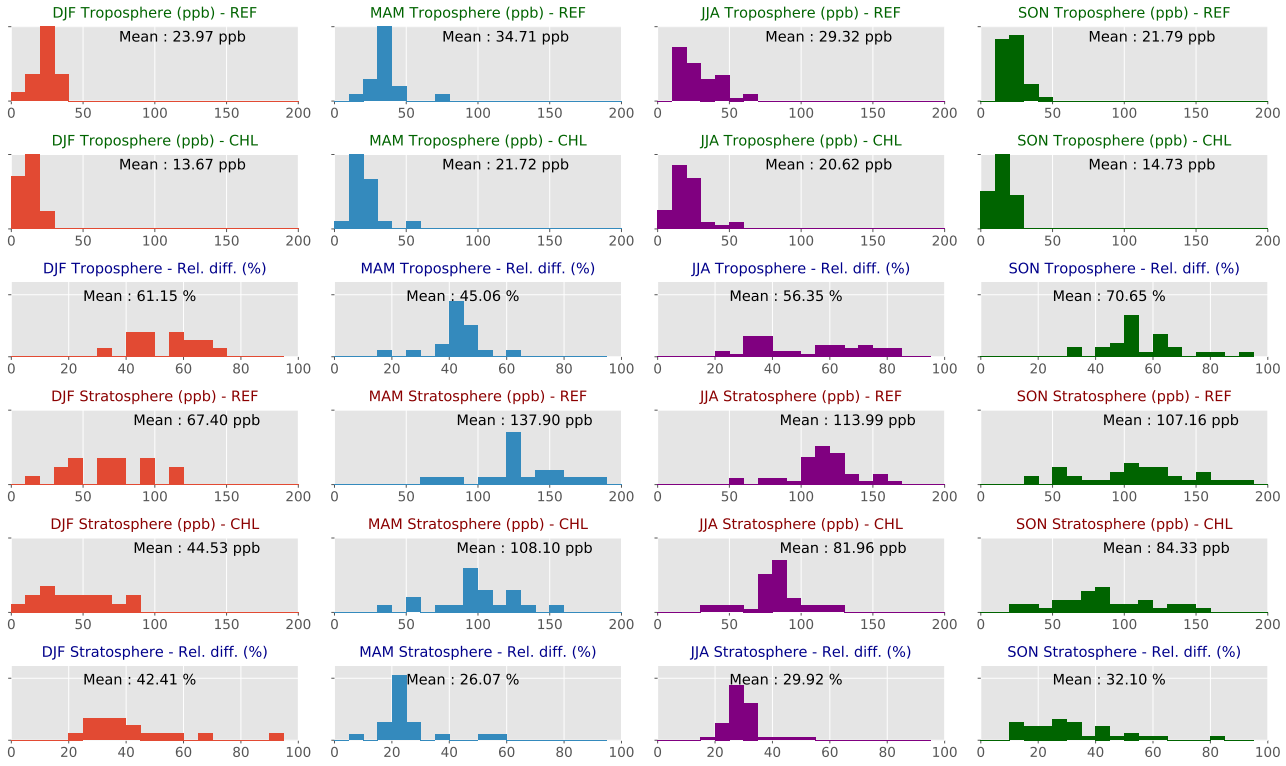

Figure 5. Distribution of the ~~difference~~ model-obs ~~over the~~ differences based on all AirCore profiles ~~. For each profile, we interpolate the model vertical profiles on the pressure grid of the profile and calculate the difference of mixing ratios. We then compute the mean of the differences~~ for ~~a specific region of~~ the ~~atmosphere. The three first lines shows the differences in the troposphere~~ four seasons (winter to fall by column) and the ~~last three ones the impact in the stratosphere~~tropospheric (1st to 3rd rows) and stratospheric (4th to 6th rows) layers . ~~The first line of each group shows~~ First and 4th row show the distribution of the absolute model-obs difference in the troposphere and stratosphere (respectively) for the REF simulations for each season (without the chlorine sink). ~~The second line shows~~ Second and 5th rows show the same for the CHL simulations (with the chlorine sink). ~~The third line shows~~ Third and 6th rows show the reduction ratio according to the equation (~~6~~5). The ~~three last lines show the same features as the three first lines but in the stratosphere. The~~ mean values calculated over the full dataset ~~is reported~~ are displayed in each frame.

3.4 Impact of Cl on stratospheric δ^{13}C-CH_4

The ~~present~~ offline version of LMDz ~~should~~ has to be able to properly simulate ~~^{13}C:^{12}C ratio~~ δ^{13}C-CH_4 values if future inversions are ~~to be~~ run with δ^{13}C-CH_4 as ~~a supplementary~~ an additional constraint. The simulated isotopic signal depends strongly on ~~the~~ estimated sinks, ~~of the isotopic signature~~ on the isotopic signatures chosen for the sources, on the relative magnitude of the sources and on ~~the~~ atmospheric transport. Among the sinks, the Cl sink is the most strongly fractionating ~~one~~ (see Table 1). Therefore, ~~even though~~ although the impact of Cl on total ~~methane~~ CH_4 is small in comparison to OH, Cl is expected to greatly influence the ~~^{13}C:^{12}C ratio~~δ^{13}C-CH_4 values, especially in regions where the Cl sink is predominant.

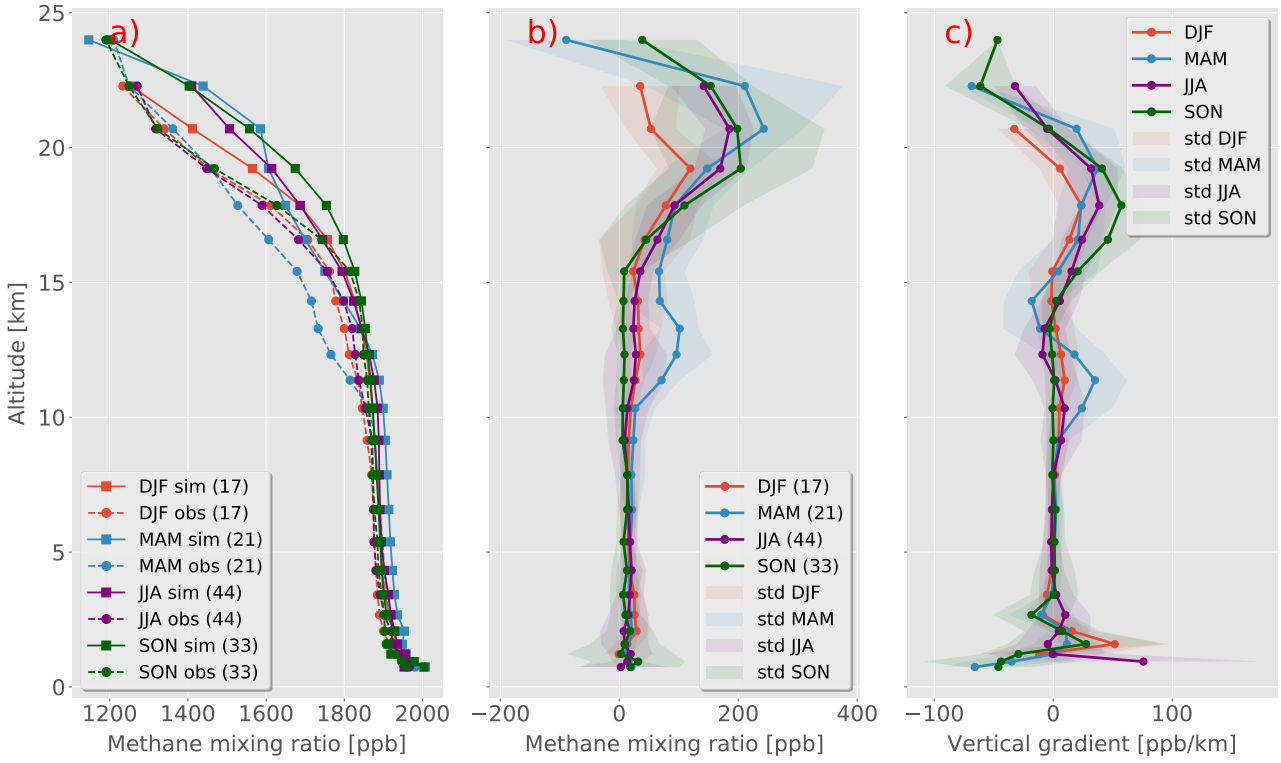

Figure 6. a) ~~Mean~~ Seasonal mean of simulated (solid lines) and observed (dashed lines) Aircore profiles in ppb. The ~~figure~~ number in ~~brackets~~ parentheses in the legend gives the number of ~~Aircore profile retrieved~~ profiles for each season. b) Absolute difference between simulated and observed profiles by season in ppb. c) Difference between vertical simulated and observed gradients (~~sim - obs~~simulated minus observed) by season in ppb/km.~~All the profiles (simulated and observed) has been averaged over each season.~~

Here we compare our simulated results to the observations from Röckmann et al. (2011) (Table 4). ~~The results of the comparison are shown on Figure 7. Implementing the Cl sink drastically improves the simulation-observation comparison. The fact that~~ Balloon measurements were performed mainly before 2000 while our study starts in 2000. As a result, we use the day of year of the flight to compare with our simulated profile in year 2000 (same day of the year). However, above 10 km, δ^{13}C-CH_4 ~~stratospheric vertical profiles improve when implementing~~ simulated profiles show no significant inter-annual variability during the 2000-2018 period and this variability is much smaller than the measurement uncertainties (generally below 0.2 ‰ above 10km). Therefore, using simulated results for year 2000 instead of the true year to compare observations above 10 km is valid. Implementing the Cl sink ~~was already demonstrated by McCarthy (2003). However, it shows that LMDz models~~ drastically improves the model-obs comparison above 10km (Figure 7), in agreement with McCarthy (2003). As a result, LMDz represents correctly the processes affecting δ^{13}C-CH_4 ~~overall in a realistic manner~~.

Nevertheless, Figure 7 suggests that there may be a remaining underestimation of the ~~13C~~ δ^{13}C-CH_4 vertical gradient in the lower stratosphere and an overestimation above. The poor representation of the Brewer-Dobson circulation highlighted in

Section 3.3 could explain this issue. Indeed, if too much ~~methane~~ CH_4 is trapped at the tropopause~~level, the ratio ^{13}C:^{12}C~~ , δ^{13}C-CH_4 values will be reduced, and then underestimated. As a result, less ~~methane~~ CH_4 is simulated above the tropopause, leading to an overestimation of ~~the ^{13}C:^{12}C ratio~~δ^{13}C-CH_4 values. Other possible explanations would be that the values taken for the KIE are not reliable ~~enough~~ at these altitudes or that Cl concentrations are poorly estimated at these levels.

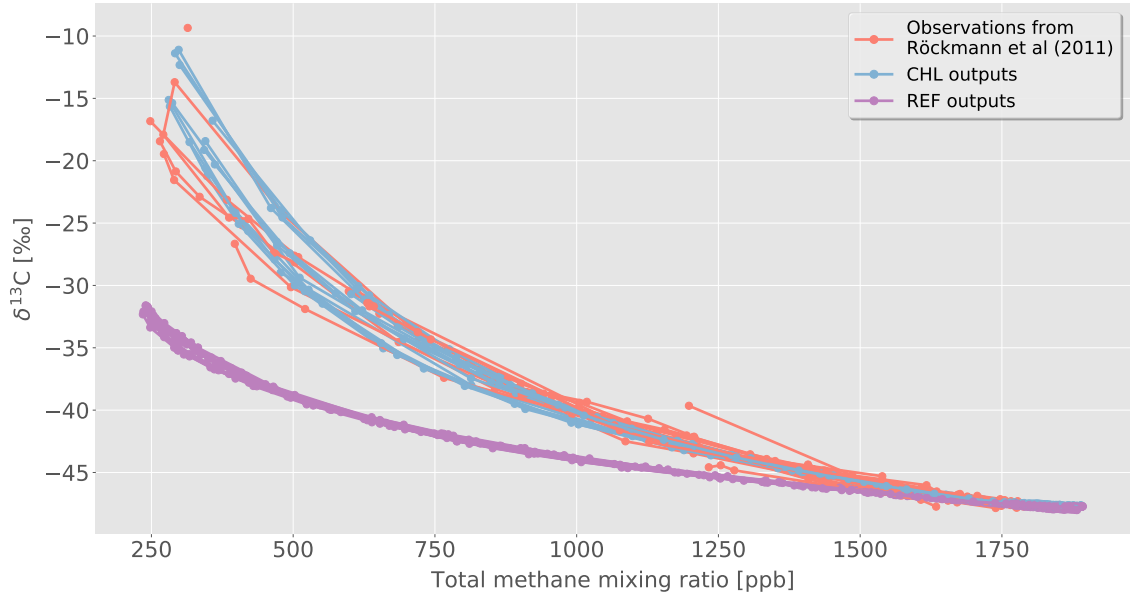

Figure 7. ~~Global mean~~ δ^{13}~~C~~ C-CH_4 values with respect to total ~~methane~~ CH_4 mixing ratio. Comparison of δ^{13}C simulations outputs with observations from Röckmann et al. (2011).

3.5 Impact of Cl on surface δ^{13}C-CH_4

To assess the impact of Cl on global surface values of δ^{13}C-CH_4, we ~~run a set of six~~ use the set of seven sensitivity tests (Table 5) ~~over the~~ spanning 2000-2018 ~~period~~ and show the ~~time series of the~~ time-series of surface global mean δ^{13}C-CH_4 signal in Figure 8.

~~Note that the initial Cl field used in the d13_CHL simulation exhibits a global tropospheric mean value of 240 atoms.cm^{-3} and a MBL mean value of 130 atoms.cm^{-3}. In the S5 scenario, the tropospheric Cl is removed. In S6, the stratospheric Cl is removed. In S7, the tropospheric global mean of Cl concentrations is scaled to 620 atoms.cm^{-3}, as reported byWang et al. (2019) . In S8, the tropospheric mean is scaled to the values of Wang et al. (2019), namely 620 atoms.cm^{-3} in the troposphere and 1200 atoms.cm^{-3} in the MBL. In S9, the Cl concentrations are decreasing by 5%/decade from 2000 to 2018. Finally, S10 is the same as the latter but with the tropospheric concentrations from Wang et al. (2019).~~ We apply the ~~same~~ transient emissions for

the entire period, ~~so the differences between the final values of each scenario are only correlated with the Cl concentrations.~~ e.g. using emissions from 2015 to simulate the year 2015.

3.5.1 Impact of tropospheric ~~chlorine~~ Cl on surface δ^{13}~~C~~C-CH_4

As expected, ~~the global surface value of~~ global-mean δ^{13}C-CH_4 surface value is found to be positively correlated with ~~the~~ Cl tropospheric mean concentration. ~~d13_REF , d13_CHL, and S7~~ As Cl reaction with CH_4 is fractionating, this sink acts to shift δ^{13}C-CH_4 towards more positive values. REF (no Cl sink), S1 (low tropospheric Cl concentrations), and S4 (high tropospheric Cl concentration) exhibit final values ~~(trend)~~ in 2018 of ~~-47.34~~ -47.44 ‰ ~~-46.98~~ , -47.09 ‰ ~~-46.78~~ , -46.92 ‰ ~~,~~ respectively. Results of ~~S8 show to what extent~~ S5 (highest tropospheric Cl concentrations) show the extent to which the MBL Cl concentrations influence ~~the surface~~ δ^{13}C-CH_4 ~~. Using~~ values at the surface. Applying a simple linear relationship between MBL concentrations and surface δ^{13}C-CH_4, we could expect a final value for ~~S8 of -45.94~~ S5 of -46.41 ‰. Instead, we obtain a final value of ~~-46.58~~ -46.73 ‰ showing that the non-linear tropospheric mixing acts to reduce the impact of MBL Cl on ~~surface~~ δ^{13}C-CH_4 at the surface. Despite this reduction, the tropospheric Cl sink shows a ~~great~~ significant influence on surface δ^{13}C-CH_4 and should be considered in forward as well as in inversions. The differences between these sensitivity simulations are much larger than observed changes in δ^{13}C-CH_4 global mean (Fig. 8). Indeed, the observed globally-averaged δ^{13}C-CH_4 trend ranges between -47,~~04~~ 10 ‰ and -47,~~38~~ 41 ‰ ~~during~~ over the 2000-2018 period (thick blue line in Fig. 8). ~~Thus the difference between d13_REF and S8~~ The difference between REF and S5 is equal to ~~250~~ 230 % of the δ^{13}C-CH_4 min-max observed range. Therefore, not considering surface Cl in an inversion can potentially lead to a significant underestimation of the weight of biogenic sources, or an overestimation of the weight of ~~anthropogenic sources (apart from livestock sectors)~~ fossil fuel sources in the global budget since the Cl sink tends to enhance δ^{13}C-CH_4 values. Simulating the same scenarios using the wetland signature map provided by Ganesan et al. (2018) ~~(a mean value of -60.8 using our fluxes) shows no significant change in the differences between the final values~~ shows similar relative results (not shown here) ~~besides shifting~~ but shifts all the values towards more negative ones (difference of -0.84 ‰ for all the final values).

~~With our wetlands isotopic signature map, the scenario giving the best agreement with observations is S6 (only tropospheric Cl) even if the post-2007 negative trend is not reproduced. With wetlands isotopic signature from Ganesan et al. (2018) (simulations not shown here), the scenario giving the best agreement with observations is S8 (Cl concentration values from Wang et al. (2019)).~~

3.5.2 Impact of stratospheric Cl on surface δ^{13}C-CH_4

The circulation in the upper troposphere and ~~the~~ lower stratosphere (UTLS) can be, to first order, described by an upwelling from the troposphere to the stratosphere in the tropics, a meridional circulation in the stratosphere to the extratropics and a downwelling from the stratosphere to the troposphere in middle and high-latitudes. (Bönisch et al., 2011; Stohl, 2003). As ~~methane~~ CH_4 is transported upward and throughout the stratosphere, it becomes heavier (less negative δ^{13}C-CH_4 values) because of fractionation of atmospheric sinks. Then, as air is injected back to the troposphere, this heavier air and the tropospheric

light air start mixing. Therefore, in addition to the enhanced δ^{13}C-CH_4 stratospheric signal, the stratospheric Cl should also have a significant impact on the tropospheric δ^{13}C-CH_4 values.

The difference between ~~the simulations d13_~~REF (no Cl at all) and ~~S5~~ S2 (no Cl in the troposphere) ~~exhibits~~ reveals the impact of stratospheric Cl through stratosphere to troposphere air injections. At the end of the ~~time series~~period, the desea-
5 sonalized trends ~~have a difference of 0.27~~ exhibits a 0.25 ‰~~.~~ difference, which represents 80% of the min-max δ^{13}C-CH_4 observed range. ~~Hence, the stratospheric Cl impact on the surface δ^{13}C-CH_4 (thus~~ Although this value has not been inferred at steady-state in the free troposphere, it is lower than the previously estimated value of 0.5 ‰ by McCarthy et al. (2001)~~)~~ ~~is~~ . Nevertheless, stratospheric Cl impact on δ^{13}C-CH_4 at the surface is still significant and running an inversion over a long time period using an isotopic constraint ~~and~~ but without implementing a realistic stratospheric Cl sink could result in ~~, for~~
10 ~~instance, an underestimation of biogenic sources intensities~~a strong underestimation of sources depleted in $^{13}CH_4$ compared to global-mean atmospheric value, i.e. less than -47.2 ‰ or, on the contrary, in an overestimation of enriched sources.

This result also raises the question of the uncertainties in the isotope source signatures. There is a 0.71 ‰ difference between a Cl-free simulation and a simulation with Cl values from Wang et al. (2019) at the end of the simulation period. Considering a 1-D box model, the final δ^{13}C-CH_4 surface value ($\delta^{13}C_{\mathrm{surf}}$) can be easily inferred from the global KIE_{app} and the mean
15 (flux- and -area weighted) signature $\delta^{13}C_{\mathrm{source}}$ using the equation below :

$$\delta^{13}C_{\mathrm{surf}} = (1 + \delta^{13}C_{\mathrm{source}}) \times \mathrm{KIE}_{\mathrm{app}} - 1 \tag{6}$$

In our simulations, $\mathrm{KIE}_{\mathrm{app}}$ is equal to about 1.0042 ± 0.0002 depending on the scenario. A difference in $\delta^{13}C_{\mathrm{source}}$ could produce the same effect as the Cl-induced shift of +0.71 ‰. This $\delta^{13}C_{\mathrm{source}}$ change could be caused by a biogenic sources intensity decrease and/or a global isotope source signature increase. For instance, increasing the isotopic signature of wetlands
20 by +2 ‰ would lead to an increase by 0.71 ‰ of $\delta^{13}C_{\mathrm{surf}}$ according to Equation (6). Hence, implementing a realistic Cl field in a poorly signature-constrained inversion would have limited impacts on the final result uncertainty. Unfortunately, wetland isotopic signatures vary widely from one study to another at the global scale, going from -60.5 ‰ (Feinberg et al., 2018) to -62 ‰ (Ganesan et al., 2018). We only discuss here the impact of global average values, as local to regional signatures can vary over much larger ranges. A box model would be too simple to rigorously study the impact of regional uncertainties.

25 ~~One possible assumption would be~~ At this stage, one possible assumption that can be formulated is that the decrease of the δ^{13}C-CH_4 since the year 2007 across the globe is not ~~completely~~ solely due to the increase of biogenic sources (Nisbet et al., 2016) but could ~~be partly~~ partly be attributed to the decrease of stratospheric reactive Cl since the Montreal Protocol. Indeed, reduced stratospheric Cl would lead to lower δ^{13}C-CH_4 surface values. Bernath and Fernando (2018) have analyzed recent observations of the stratospheric HCl mixing ratio and concluded that it decreases by about 5% ~~/decade. Even though~~
30 per decade. Although HCl (or total Cl) and atomic Cl are not so simply correlated, applying the same decrease to our Cl field could give us some insight into the potential impact of a recent decrease in stratospheric Cl on δ^{13}C-CH_4 values at the surface. ~~The scenario S9~~ S6 (low tropospheric Cl and decreasing stratospheric Cl) shows a reduction of the surface δ^{13}C-CH_4 value of only ~~0.02~~ 0.016 ‰ compared to ~~the scenario d13_CHL and the scenario S10~~ S1, and S7 (high tropospheric Cl and decreasing

stratospheric Cl) shows a reduction of ~~0.03~~ 0.038 ‰ compared to ~~S8~~S5. Hence, this shift resulting from the Montreal Protocol ratification is not likely to be ~~a~~ the major cause of the recent decrease of δ^{13}C-CH_4 values towards more negative values (about 0.3 ‰ over the last 10 years, Nisbet et al., 2019).

~~All things considered, if δ^{13}C-CH_4 constraint are to be used for sources characterization in long-period inversion runs, the simulated stratospheric impact of 0.27 when including stratospheric Cl sink should be considered.~~

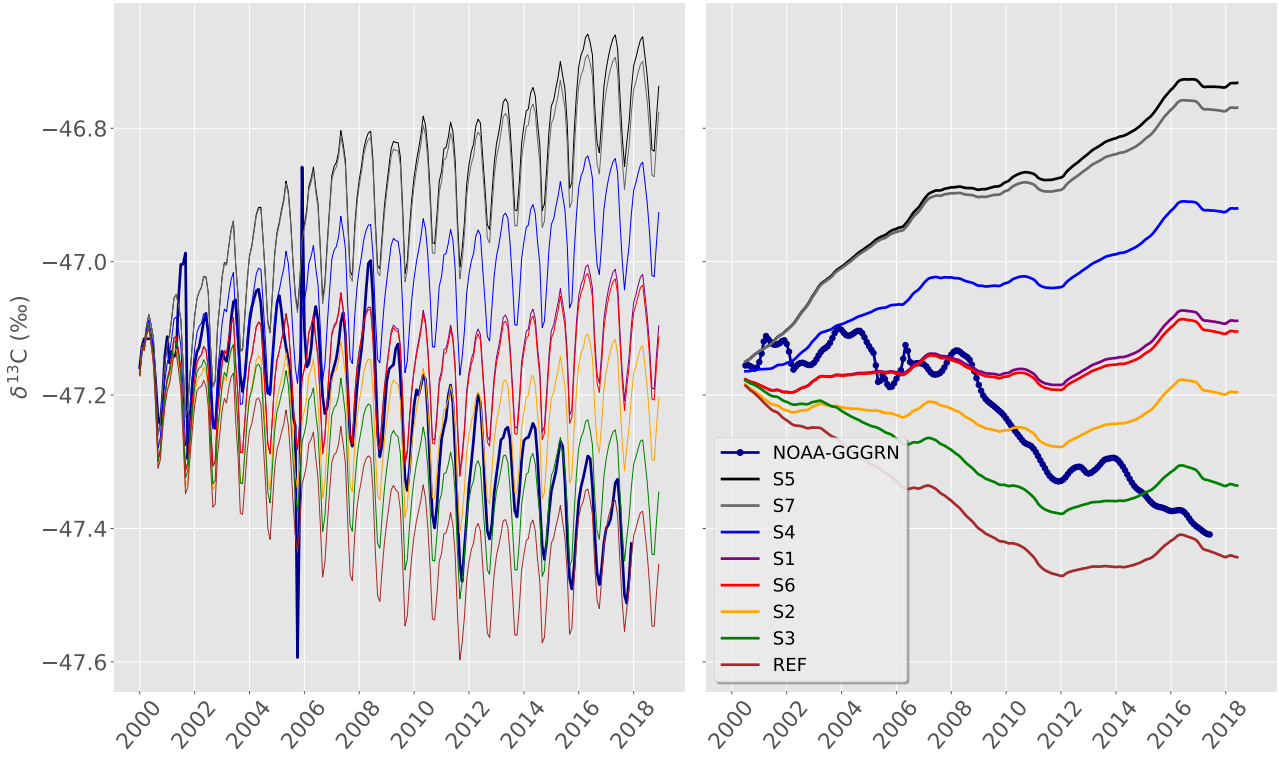

Figure 8. Time series of surface δ^{13}~~C~~ C-CH_4 global mean value for multiple scenarios. ~~Dashed lines are~~ The left panel shows the observed and simulated monthly values~~and solid lines are~~ . The right panel displays the associated deseasonalized trends. The globally-averaged NOAA-GGGRN δ^{13}~~C~~ C-CH_4 record is in dark blue. ~~The shaded area represent~~ Only MBL sites (i.e. samples from the ~~standard deviation~~ site are predominantly of well-mixed MBL air) are used here. Extreme values in 2001 and 2005 are explained by a lack of monthly values either in the ~~observed records~~North (2001-09, 2005-12) or the South Hemisphere (2001-06, 2001-07, 2005-10, 2005-11). However, this lack of data cannot explain the peak in 2008.

4 Conclusions

This study ~~presents~~ presented the impact of atomic Cl on the modeling of total ~~methane~~ CH_4 removal and on δ^{13}C-CH_4 using the 3-D GCM LMDz. Three ~~methane observational datasets have been~~ CH_4 observational datasets were used to assess this impact: 115 AirCore vertical profiles, δ^{13}C-CH_4 stratospheric measurements from Röckmann et al. (2011) and δ^{13}C-

CH_4 2000-2018 records from ~~18~~ 11 ground stations distributed all over the world. ~~10~~ Seven forward simulations (including 6 sensitivity ~~test runs) have been assessing~~ tests) were carried out to assess the impact of Cl field on ~~methane simulated concentrations.~~ CH_4 simulated mixing ratios.

The Cl stratospheric sink strength ~~is~~ was estimated to be 7.16 ± ~~0.27~~ 0.26 Tg/yr, accounting for 29% of the total stratospheric sink. Implementing the Cl sink ~~has also an effect on methane total column~~ affected CH_4 total columns (XCH_4) ~~of about 1% (18~~ by about 1.2% (21.9 ppb) after a ~~13-year~~ 19-year simulation period (~~2006-2018). Even though the Cl sink reduces~~ 2000-2018). Although including this Cl sink reduced the discrepancies between AirCore and simulated ~~methane~~ CH_4 vertical profiles, large discrepancies in both tropospheric (likely mostly due to the non-optimized emission scenario) and stratospheric CH_4 still remain. ~~LMDz has difficulties to reproduce small-scale variations~~ In particular, LMDz is not able to reproduce very localized mixing ratio spikes exhibited during boreal spring and summer. Moreover, the Brewer-Dobson circulation that governs lower to upper stratosphere air transport is only fairly reproduced in our model. We also showed that ~~the isotopic ratio ^{13}C:^{12}C ratio is~~ δ^{13}C-CH_4 values are more substantially affected by ~~the Cl than total~~ Cl than CH_4 ~~. The stratospheric vertical profiles of~~ mixing ratio. Simulated δ^{13}C-CH_4 ~~values~~ stratospheric vertical profiles agree very well with observations from Röckmann et al. (2011) when including the Cl sink. ~~At the surface, the set of the~~ The set of sensitivity tests performed with or without ~~the~~ stratospheric or tropospheric Cl sink show that ~~the Cl concentrations at the surface~~ tropospheric and MBL Cl concentrations can largely affect ~~the~~ δ^{13}C-CH_4 ~~surface signal~~ signal at the surface. Indeed, there is a difference of ~~0.76~~ 0.71 ‰ between a Cl-free simulation and a simulation with Cl values from Wang et al. (2019) ~~(last values of each detrended time series). This influence~~ in 2018. This result also raises the question of the uncertainties on the ~~source isotopic signatures. Considering a 1-D model, the final δ^{13}C-CH_4 surface value ($\delta^{13}C_{surf}$) can be easily inferred from the global KIEapp and the mean (flux- and -area weighted) signature $\delta^{13}C_{source}$ using the equation below :~~

~~$\delta^{13}C_{surf} = (1 + \delta^{13}C_{source}) \times KIE_{app} - 1$~~

isotope source signatures.

~~A δ^{13}C-CH_4 source delta (difference) could produce the same effect as the Cl-induced shift of 0.76 . This $\delta^{13}C_{source}$ change could be caused by a decrease in the biogenic sources intensities and/or an increase in these sources isotopic signatures. Taking the example of wetlands in our study, decreasing the share of the wetlands in the total budget of 7% or increasing the isotopic signature of +2 would lead to a 0.76 $\delta^{13}C_{source}$ increase. Hence, implementing a realistic Cl field in a poorly signature-constrained inversion would have limited impacts on the final result uncertainty. Unfortunately, wetland isotopic signatures vary widely from one study to another at the global scale, going from -60.5 Feinberg et al. (2018) to -62 Ganesan et al. (2018 and we only discuss here the impact of global average values, as local to regional signatures can vary over much larger ranges. A box model would be too simple to rigorously study the impact of regional uncertainties.~~ In addition, the stratospheric impact of Cl on surface δ^{13}C-CH_4 values ~~is~~ was found to be as high as ~~0.27~~ 0.25 ‰~~.~~ with our model and the associated setup, and hence of the same magnitude as recorded variations of δ^{13}C-CH_4 in the past decade. However, ~~recent Cl concentration decrease~~

the recent decrease in Cl concentration in the stratosphere owing to the Montreal Protocol ~~are~~ is not likely an explanation for the recent shift of δ^{13}C-CH_4 values towards more negative values.

~~We should also not ignore the errors~~ Finaly, errors remain in the estimation of ~~total methane in~~ CH_4 mixing ratios in the UTLS. This problem has been resolved by some ~~modellers~~ modelling groups by implementing isentropic coordinates, best suited for Brewer-Dobson circulation representation, but are unlikely to be ~~done~~ implemented in LMDz in the near future due to technical considerations~~and a~~. A way to virtually move ~~methane upwards~~ CH_4 into the upper stratosphere should be ~~rather~~ considered. Future work will focus on running inversions with isotopic constraints to better characterize the various ~~methane~~ CH_4 sources and sinks, with the use of ~~spatially resolved~~ spatially-resolved isotopic signature maps as suggested by Feinberg et al. (2018) and Ganesan et al. (2018) in order to limit the errors generated by a poor representation of these elements. Some sensitivity tests using different OH and Cl fields should be also considered in order to quantify the impact of sinks uncertainties on inversion results.

Data availability. The data for δ^{13}C-CH_4 observations were downloaded from the World Data Centre for Greenhouse Gases (WDCGG) at https://gaw.kishou.go.jp. Datasets for the input emissions were provided by the Global Carbon Project (GCP) team. The AirCore vertical profiles from the NOAA-ESRL Aircraft Program (v20181101) were provided by CS and BB. The Cl fields, the modelling output files and the AirCore vertical profiles from the French AirCore Program are available upon request from the corresponding author.

Author contributions. JT designed and run the simulation experiments and performed the data analysis presented in this paper. DH provided the Cl fields used for the simulations. The AirCore data was retrieved and provided by MR and CR (from the French AirCore Team) and CS and BB (from the NOAA-ESRL Aircraft Program, v20181101). MS provided the total CH_4 fluxes. MS, AB, IP and PB provided scientific and technical expertise. They also contributed to the scientific analysis of this work. JT prepared the manuscript with contributions from all co-authors.

Competing interests. The authors declare that they have no conflict of interest.

Acknowledgements. This work was supported by the CEA (Commissariat à l'Energie Atomique et aux Energies Alternatives). We thank both reviewers for their helpful suggestions and comments. We are grateful to Thomas Röckmann for sharing his data and for insightful discussion. The study extensively relies on the meteorological data provided by the ECMWF. Calculations were performed using the computing resources of LSCE, maintained by François Marabelle and the LSCE IT team. The authors wish to thank the measurement teams from the Global Greenhouse Gas Reference Network (NOAA) for their work.

References

Allan, W.: Interannual variation of ^{13} C in tropospheric methane: Implications for a possible atomic chlorine sink in the marine boundary layer, Journal of Geophysical Research, 110, https://doi.org/10.1029/2004JD005650, http://doi.wiley.com/10.1029/2004JD005650, 2005.

Allan, W., Lowe, D. C., and Cainey, J. M.: Active chlorine in the remote marine boundary layer: Modeling anomalous measurements of 13C in methane, Geophysical Research Letters, 28, 3239–3242, https://doi.org/10.1029/2001GL013064, https://agupubs.pericles-prod.literatumonline.com/doi/abs/10.1029/2001GL013064, 2001.

Allan, W., Struthers, H., and Lowe, D. C.: Methane carbon isotope effects caused by atomic chlorine in the marine boundary layer: Global model results compared with Southern Hemisphere measurements, Journal of Geophysical Research, 112, https://doi.org/10.1029/2006JD007369, http://doi.wiley.com/10.1029/2006JD007369, 2007.

Bergamaschi, P., Karstens, U., Manning, A. J., Saunois, M., Tsuruta, A., Berchet, A., Vermeulen, A. T., Arnold, T., Janssens-Maenhout, G., Hammer, S., Levin, I., Schmidt, M., Ramonet, M., Lopez, M., Lavric, J., Aalto, T., Chen, H., Feist, D. G., Gerbig, C., Haszpra, L., Hermansen, O., Manca, G., Moncrieff, J., Meinhardt, F., Necki, J., Galkowski, M., O'Doherty, S., Paramonova, N., Scheeren, H. A., Steinbacher, M., and Dlugokencky, E.: Inverse modelling of European CH_4 emissions during 2006–2012 using different inverse models and reassessed atmospheric observations, Atmospheric Chemistry and Physics, 18, 901–920, https://doi.org/https://doi.org/10.5194/acp-18-901-2018, https://www.atmos-chem-phys.net/18/901/2018/, 2018.

Bernath, P. and Fernando, A. M.: Trends in stratospheric HCl from the ACE satellite mission, Journal of Quantitative Spectroscopy and Radiative Transfer, 217, 126–129, https://doi.org/10.1016/j.jqsrt.2018.05.027, http://www.sciencedirect.com/science/article/pii/S0022407317309548, 2018.

Bousquet, P., Ciais, P., Miller, J. B., Dlugokencky, E. J., Hauglustaine, D. A., Prigent, C., Van der Werf, G. R., Peylin, P., Brunke, E.-G., Carouge, C., Langenfelds, R. L., Lathière, J., Papa, F., Ramonet, M., Schmidt, M., Steele, L. P., Tyler, S. C., and White, J.: Contribution of anthropogenic and natural sources to atmospheric methane variability, Nature, 443, 439–443, https://doi.org/10.1038/nature05132, http://www.nature.com/articles/nature05132, 2006.

Burkholder, J. B., Abbatt, J. P. D., Huie, R. E., Kurylo, M. J., Wilmouth, D. M., Sander, S. P., Barker, J. R., Kolb, C. E., Orkin, V. L., and Wine, P. H.: JPL Publication 15-10: Chemical Kinetics and Photochemical Data for Use in Atmospheric Studies, p. 1392, 2015.

Bönisch, H., Engel, A., Birner, T., Hoor, P., Tarasick, D. W., and Ray, E. A.: On the structural changes in the Brewer-Dobson circulation after 2000, Atmospheric Chemistry and Physics, 11, 3937–3948, https://doi.org/https://doi.org/10.5194/acp-11-3937-2011, https://www.atmos-chem-phys.net/11/3937/2011/, 2011.

Chevallier, F., Fisher, M., Peylin, P., Serrar, S., Bousquet, P., Bréon, F.-M., Chédin, A., and Ciais, P.: Inferring CO_2 sources and sinks from satellite observations: Method and application to TOVS data, Journal of Geophysical Research, 110, https://doi.org/10.1029/2005JD006390, http://doi.wiley.com/10.1029/2005JD006390, 2005.

Craig, H.: Isotopic standards for carbon and oxygen and correction factors for mass-spectrometric analysis of carbon dioxide, Geochimica et Cosmochimica Acta, 12, 133–149, https://doi.org/10.1016/0016-7037(57)90024-8, http://www.sciencedirect.com/science/article/pii/0016703757900248, 1957.

Etheridge, D. M., Steele, L. P., Francey, R. J., and Langenfelds, R. L.: Atmospheric methane between 1000 A.D. and present: Evidence of anthropogenic emissions and climatic variability, Journal of Geophysical Research: Atmospheres, 103, 15 979–15 993, https://doi.org/10.1029/98JD00923, http://doi.wiley.com/10.1029/98JD00923, 1998.

Etiope, G.: Natural Gas Seepage: The Earth's Hydrocarbon Degassing, Springer International Publishing, https://www.springer.com/gp/book/9783319146003, 2015.

Feinberg, A. I., Coulon, A., Stenke, A., Schwietzke, S., and Peter, T.: Isotopic source signatures: Impact of regional variability on the 13CH4 trend and spatial distribution, Atmospheric Environment, 174, 99–111, https://doi.org/10.1016/j.atmosenv.2017.11.037, http://www.sciencedirect.com/science/article/pii/S1352231017307902, 2018.

Folberth, G. A., Hauglustaine, D. A., Lathière, J., and Brocheton, F.: Interactive chemistry in the Laboratoire de Météorologie Dynamique general circulation model: model description and impact analysis of biogenic hydrocarbons on tropospheric chemistry, Atmospheric Chemistry and Physics, 6, 2273–2319, https://doi.org/10.5194/acp-6-2273-2006, http://www.atmos-chem-phys.net/6/2273/2006/, 2006.

Ganesan, A. L., Stell, A. C., Gedney, N., Comyn-Platt, E., Hayman, G., Rigby, M., Poulter, B., and Hornibrook, E. R. C.: Spatially Resolved Isotopic Source Signatures of Wetland Methane Emissions, Geophysical Research Letters, 45, 3737–3745, https://doi.org/10.1002/2018GL077536, https://agupubs.onlinelibrary.wiley.com/doi/abs/10.1002/2018GL077536, 2018.

Gromov, S., Brenninkmeijer, C. A. M., and Jöckel, P.: A very limited role of tropospheric chlorine as a sink of the greenhouse gas methane, Atmospheric Chemistry and Physics, 18, 9831–9843, https://doi.org/https://doi.org/10.5194/acp-18-9831-2018, https://www.atmos-chem-phys.net/18/9831/2018/, 2018.

Gupta, M., Tyler, S., and Cicerone, R.: Modeling atmospheric 13CH4 and the causes of recent changes in atmospheric CH4 amounts, Journal of Geophysical Research: Atmospheres, 101, 22 923–22 932, https://doi.org/10.1029/96JD02386, https://agupubs.onlinelibrary.wiley.com/doi/abs/10.1029/96JD02386, 1996.

Hauglustaine, D. A., Hourdin, F., Jourdain, L., Filiberti, M.-A., Walters, S., Lamarque, J.-F., and Holland, E. A.: Interactive chemistry in the Laboratoire de Météorologie Dynamique general circulation model: Description and background tropospheric chemistry evaluation, Journal of Geophysical Research: Atmospheres, 109, https://doi.org/10.1029/2003JD003957, https://agupubs.onlinelibrary.wiley.com/doi/full/10.1029/2003JD003957, 2004.

Hossaini, R., Chipperfield, M. P., Saiz-Lopez, A., Fernandez, R., Monks, S., Feng, W., Brauer, P., and von Glasow, R.: A global model of tropospheric chlorine chemistry: Organic versus inorganic sources and impact on methane oxidation, Journal of Geophysical Research: Atmospheres, 121, 14,271–14,297, https://doi.org/10.1002/2016JD025756, https://agupubs.onlinelibrary.wiley.com/doi/full/10.1002/2016JD025756, 2016.

Hourdin, F., Musat, I., Bony, S., Braconnot, P., Codron, F., Dufresne, J.-L., Fairhead, L., Filiberti, M.-A., Friedlingstein, P., Grandpeix, J.-Y., Krinner, G., LeVan, P., Li, Z.-X., and Lott, F.: The LMDZ4 general circulation model: climate performance and sensitivity to parametrized physics with emphasis on tropical convection, Climate Dynamics, 27, 787–813, https://doi.org/10.1007/s00382-006-0158-0, http://link.springer.com/10.1007/s00382-006-0158-0, 2006.

Janssens-Maenhout, G., Crippa, M., Guizzardi, D., Muntean, M., Schaaf, E., Dentener, F., Bergamaschi, P., Pagliari, V., Olivier, J. G. J., Peters, J. A. H. W., Aardenne, J. A. v., Monni, S., Doering, U., and Petrescu, A. M. R.: EDGAR v4.3.2 Global Atlas of the three major Greenhouse Gas Emissions for the period 1970–2012, Earth System Science Data Discussions, pp. 1–55, https://doi.org/https://doi.org/10.5194/essd-2017-79, https://www.earth-syst-sci-data-discuss.net/essd-2017-79/, 2017.

Karion, A., Sweeney, C., Tans, P., and Newberger, T.: AirCore: An Innovative Atmospheric Sampling System, Journal of Atmospheric and Oceanic Technology, 27, 1839–1853, https://doi.org/10.1175/2010JTECHA1448.1, https://journals.ametsoc.org/doi/full/10.1175/2010JTECHA1448.1, 2010.

King, S. L., Quay, P. D., and Lansdown, J. M.: The 13C/12C kinetic isotope effect for soil oxidation of methane at ambient atmospheric concentrations, Journal of Geophysical Research: Atmospheres, 94, 18 273–18 277, https://doi.org/10.1029/JD094iD15p18273, http://agupubs.onlinelibrary.wiley.com/doi/abs/10.1029/JD094iD15p18273, 1989.

Kirschke, S., Bousquet, P., Ciais, P., Saunois, M., Canadell, J. G., Dlugokencky, E. J., Bergamaschi, P., Bergmann, D., Blake, D. R., Bruhwiler, L., Cameron-Smith, P., Castaldi, S., Chevallier, F., Feng, L., Fraser, A., Heimann, M., Hodson, E. L., Houweling, S., Josse, B., Fraser, P. J., Krummel, P. B., Lamarque, J.-F., Langenfelds, R. L., Le Quéré, C., Naik, V., O'Doherty, S., Palmer, P. I., Pison, I., Plummer, D., Poulter, B., Prinn, R. G., Rigby, M., Ringeval, B., Santini, M., Schmidt, M., Shindell, D. T., Simpson, I. J., Spahni, R., Steele, L. P., Strode, S. A., Sudo, K., Szopa, S., van der Werf, G. R., Voulgarakis, A., van Weele, M., Weiss, R. F., Williams, J. E., and Zeng, G.: Three decades of global methane sources and sinks, Nature Geoscience, 6, 813–823, https://doi.org/10.1038/ngeo1955, http://www.nature.com/articles/ngeo1955, 2013.

Lambert, G. and Schmidt, S.: Reevaluation of the oceanic flux of methane: Uncertainties and long term variations, Chemosphere, 26, 579–589, https://doi.org/10.1016/0045-6535(93)90443-9, http://www.sciencedirect.com/science/article/pii/0045653593904439, 1993.

Locatelli, R., Bousquet, P., Hourdin, F., Saunois, M., Cozic, A., Couvreux, F., Grandpeix, J.-Y., Lefebvre, M.-P., Rio, C., Bergamaschi, P., Chambers, S. D., Karstens, U., Kazan, V., van der Laan, S., Meijer, H. A. J., Moncrieff, J., Ramonet, M., Scheeren, H. A., Schlosser, C., Schmidt, M., Vermeulen, A., and Williams, A. G.: Atmospheric transport and chemistry of trace gases in LMDz5B: evaluation and implications for inverse modelling, Geoscientific Model Development, 8, 129–150, https://doi.org/10.5194/gmd-8-129-2015, https://www.geosci-model-dev.net/8/129/2015/, 2015a.

Locatelli, R., Bousquet, P., Saunois, M., Chevallier, F., and Cressot, C.: Sensitivity of the recent methane budget to LMDz sub-grid-scale physical parameterizations, Atmospheric Chemistry and Physics, 15, 9765–9780, https://doi.org/10.5194/acp-15-9765-2015, http://www.atmos-chem-phys.net/15/9765/2015/, 2015b.

Louis, J.-F.: A parametric model of vertical eddy fluxes in the atmosphere, Boundary-Layer Meteorology, 17, 187–202, https://doi.org/10.1007/BF00117978, https://doi.org/10.1007/BF00117978, 1979.

Marécal, V., Peuch, V.-H., Andersson, C., Andersson, S., Arteta, J., Beekmann, M., Benedictow, A., Bergström, R., Bessagnet, B., Cansado, A., Chéroux, F., Colette, A., Coman, A., Curier, R. L., Denier van der Gon, H. a. C., Drouin, A., Elbern, H., Emili, E., Engelen, R. J., Eskes, H. J., Foret, G., Friese, E., Gauss, M., Giannaros, C., Guth, J., Joly, M., Jaumouillé, E., Josse, B., Kadygrov, N., Kaiser, J. W., Krajsek, K., Kuenen, J., Kumar, U., Liora, N., Lopez, E., Malherbe, L., Martinez, I., Melas, D., Meleux, F., Menut, L., Moinat, P., Morales, T., Parmentier, J., Piacentini, A., Plu, M., Poupkou, A., Queguiner, S., Robertson, L., Rouïl, L., Schaap, M., Segers, A., Sofiev, M., Tarasson, L., Thomas, M., Timmermans, R., Valdebenito, , van Velthoven, P., van Versendaal, R., Vira, J., and Ung, A.: A regional air quality forecasting system over Europe: the MACC-II daily ensemble production, Geoscientific Model Development, 8, 2777–2813, https://doi.org/https://doi.org/10.5194/gmd-8-2777-2015, https://www.geosci-model-dev.net/8/2777/2015/, 2015.

McCarthy, M. C.: Carbon and hydrogen isotopic compositions of stratospheric methane: 2. Two-dimensional model results and implications for kinetic isotope effects, Journal of Geophysical Research, 108, https://doi.org/10.1029/2002JD003183, http://doi.wiley.com/10.1029/2002JD003183, 2003.

McCarthy, M. C., Connell, P., and Boering, K. A.: Isotopic fractionation of methane in the stratosphere and its effect on free tropospheric isotopic compositions, Geophysical Research Letters, 28, 3657–3660, https://doi.org/10.1029/2001GL013159, https://agupubs.onlinelibrary.wiley.com/doi/abs/10.1029/2001GL013159, 2001.

McNorton, J., Wilson, C., Gloor, M., Parker, R. J., Boesch, H., Feng, W., Hossaini, R., and Chipperfield, M. P.: Attribution of recent increases in atmospheric methane through 3-D inverse modelling, Atmospheric Chemistry and Physics, 18, 18 149–18 168, https://doi.org/https://doi.org/10.5194/acp-18-18149-2018, https://www.atmos-chem-phys.net/18/18149/2018/, 2018.

Meinshausen, M., Vogel, E., Nauels, A., Lorbacher, K., Meinshausen, N., Etheridge, D. M., Fraser, P. J., Montzka, S. A., Rayner, P. J., Trudinger, C. M., Krummel, P. B., Beyerle, U., Canadell, J. G., Daniel, J. S., Enting, I. G., Law, R. M., Lunder, C. R., O'Doherty, S., Prinn, R. G., Reimann, S., Rubino, M., Velders, G. J. M., Vollmer, M. K., Wang, R. H. J., and Weiss, R.: Historical greenhouse gas concentrations for climate modelling (CMIP6), Geoscientific Model Development, 10, 2057–2116, https://doi.org/https://doi.org/10.5194/gmd-10-2057-2017, https://www.geosci-model-dev.net/10/2057/2017/, 2017.

Membrive, O., Crevoisier, C., Sweeney, C., Danis, F., Hertzog, A., Engel, A., Bönisch, H., and Picon, L.: AirCore-HR: a high-resolution column sampling to enhance the vertical description of CH4 and CO2, Atmos. Meas. Tech., p. 20, 2017.

Menut, L., Bessagnet, B., Khvorostyanov, D., Beekmann, M., Blond, N., Colette, A., Coll, I., Curci, G., Foret, G., Hodzic, A., Mailler, S., Meleux, F., Monge, J.-L., Pison, I., Siour, G., Turquety, S., Valari, M., Vautard, R., and Vivanco, M. G.: CHIMERE 2013: a model for regional atmospheric composition modelling, Geoscientific Model Development, 6, 981–1028, https://doi.org/10.5194/gmd-6-981-2013, https://www.geosci-model-dev.net/6/981/2013/, 2013.

Monteil, G., Houweling, S., Dlugockenky, E. J., Maenhout, G., Vaughn, B. H., White, J. W. C., and Rockmann, T.: Interpreting methane variations in the past two decades using measurements of CH_4 mixing ratio and isotopic composition, Atmospheric Chemistry and Physics, 11, 9141–9153, https://doi.org/https://doi.org/10.5194/acp-11-9141-2011, https://www.atmos-chem-phys.net/11/9141/2011/acp-11-9141-2011.html, 2011.

Müller, R., Brenninkmeijer, C. A. M., and Crutzen, P. J.: A Large 13CO deficit in the lower Antarctic stratosphere due to "ozone hole" chemistry: Part II, Modeling, Geophysical Research Letters, 23, 2129–2132, https://doi.org/10.1029/96GL01472, http://agupubs.onlinelibrary.wiley.com/doi/abs/10.1029/96GL01472, 1996.

Nakajima, H., Wohltmann, I., Wegner, T., Takeda, M., Pitts, M. C., Poole, L. R., Lehmann, R., Santee, M. L., and Rex, M.: Polar stratospheric cloud evolution and chlorine activation measured by CALIPSO and MLS, and modeled by ATLAS, Atmospheric Chemistry and Physics, 16, 3311–3325, https://doi.org/10.5194/acp-16-3311-2016, https://www.atmos-chem-phys.net/16/3311/2016/, 2016.

Nassar, R., Bernath, P. F., Boone, C. D., Clerbaux, C., Coheur, P. F., Dufour, G., Froidevaux, L., Mahieu, E., McConnell, J. C., McLeod, S. D., Murtagh, D. P., Rinsland, C. P., Semeniuk, K., Skelton, R., Walker, K. A., and Zander, R.: A global inventory of stratospheric chlorine in 2004, Journal of Geophysical Research, 111, https://doi.org/10.1029/2006JD007073, http://doi.wiley.com/10.1029/2006JD007073, 2006.

Neef, L., Weele, M. v., and Velthoven, P. v.: Optimal estimation of the present-day global methane budget, Global Biogeochemical Cycles, 24, https://doi.org/10.1029/2009GB003661, https://agupubs.onlinelibrary.wiley.com/doi/abs/10.1029/2009GB003661, 2010.

Nisbet, E. G., Dlugokencky, E. J., Manning, M. R., Lowry, D., Fisher, R. E., France, J. L., Michel, S. E., Miller, J. B., White, J. W. C., Vaughn, B., Bousquet, P., Pyle, J. A., Warwick, N. J., Cain, M., Brownlow, R., Zazzeri, G., Lanoisellé, M., Manning, A. C., Gloor, E., Worthy, D. E. J., Brunke, E.-G., Labuschagne, C., Wolff, E. W., and Ganesan, A. L.: Rising atmospheric methane: 2007-2014 growth and isotopic shift: RISING METHANE 2007-2014, Global Biogeochemical Cycles, 30, 1356–1370, https://doi.org/10.1002/2016GB005406, http://doi.wiley.com/10.1002/2016GB005406, 2016.

Nisbet, E. G., Manning, M. R., Dlugokencky, E. J., Fisher, R. E., Lowry, D., Michel, S. E., Myhre, C. L., Platt, S. M., Allen, G., Bousquet, P., Brownlow, R., Cain, M., France, J. L., Hermansen, O., Hossaini, R., Jones, A. E., Levin, I., Manning, A. C., Myhre, G., Pyle, J. A., Vaughn, B. H., Warwick, N. J., and White, J. W. C.: Very Strong Atmospheric Methane Growth in the 4 Years 2014–2017: Implications for

the Paris Agreement, Global Biogeochemical Cycles, 33, 318–342, https://doi.org/10.1029/2018GB006009, https://agupubs.onlinelibrary.wiley.com/doi/abs/10.1029/2018GB006009, 2019.

Patra, P. K., Houweling, S., Krol, M., Bousquet, P., Belikov, D., Bergmann, D., Bian, H., Cameron-Smith, P., Chipperfield, M. P., Corbin, K., Fortems-Cheiney, A., Fraser, A., Gloor, E., Hess, P., Ito, A., Kawa, S. R., Law, R. M., Loh, Z., Maksyutov, S., Meng, L., Palmer, P. I., Prinn, R. G., Rigby, M., Saito, R., and Wilson, C.: TransCom model simulations of CH_4 and related species: linking transport, surface flux and chemical loss with CH_4 variability in the troposphere and lower stratosphere, Atmospheric Chemistry and Physics, 11, 12 813–12 837, https://doi.org/10.5194/acp-11-12813-2011, http://www.atmos-chem-phys.net/11/12813/2011/, 2011.

Pison, I., Bousquet, P., Chevallier, F., Szopa, S., and Hauglustaine, D.: Multi-species inversion of CH4, CO and H2 emissions from surface measurements, Atmos. Chem. Phys., p. 17, 2009.

Poulter, B., Bousquet, P., Canadell, J. G., Ciais, P., Peregon, A., Saunois, M., Arora, V. K., Beerling, D. J., Brovkin, V., Jones, C. D., Joos, F., Gedney, N., Ito, A., Kleinen, T., Koven, C. D., McDonald, K., Melton, J. R., Peng, C., Peng, S., Prigent, C., Schroeder, R., Riley, W. J., Saito, M., Spahni, R., Tian, H., Taylor, L., Viovy, N., Wilton, D., Wiltshire, A., Xu, X., Zhang, B., Zhang, Z., and Zhu, Q.: Global wetland contribution to 2000–2012 atmospheric methane growth rate dynamics, Environmental Research Letters, 12, 094 013, https://doi.org/10.1088/1748-9326/aa8391, https://doi.org/10.1088%2F1748-9326%2Faa8391, 2017.

Reeburgh, W. S., Hirsch, A. I., Sansone, F. J., Popp, B. N., and Rust, T. M.: Carbon kinetic isotope effect accompanying microbial oxidation of methane in boreal forest soils, Geochimica et Cosmochimica Acta, 61, 4761–4767, https://doi.org/10.1016/S0016-7037(97)00277-9, http://www.sciencedirect.com/science/article/pii/S0016703797002779, 1997.

Rice, A. L., Butenhoff, C. L., Teama, D. G., Röger, F. H., Khalil, M. A. K., and Rasmussen, R. A.: Atmospheric methane isotopic record favors fossil sources flat in 1980s and 1990s with recent increase, Proceedings of the National Academy of Sciences, 113, 10 791–10 796, https://doi.org/10.1073/pnas.1522923113, https://www.pnas.org/content/113/39/10791, 2016.

Ridgwell, A. J., Marshall, S. J., and Gregson, K.: Consumption of atmospheric methane by soils: A process-based model, Global Biogeochemical Cycles, 13, 59–70, https://doi.org/10.1029/1998GB900004, http://doi.wiley.com/10.1029/1998GB900004, 1999.

Röckmann, T., Grooß, J.-U., and Müller, R.: The impact of anthropogenic chlorine emissions, stratospheric ozone change and chemical feedbacks on stratospheric water, Atmospheric Chemistry and Physics, 4, 693–699, https://doi.org/10.5194/acp-4-693-2004, http://www.atmos-chem-phys.net/4/693/2004/, 2004.

Röckmann, T., Brass, M., Borchers, R., and Engel, A.: The isotopic composition of methane in the stratosphere: high-altitude balloon sample measurements, Atmospheric Chemistry and Physics, 11, 13 287–13 304, https://doi.org/https://doi.org/10.5194/acp-11-13287-2011, https://www.atmos-chem-phys.net/11/13287/2011/, 2011.

Saueressig, G., Bergamaschi, P., Crowley, J. N., Fischer, H., and Harris, G. W.: Carbon kinetic isotope effect in the reaction of CH4 with Cl atoms, Geophysical Research Letters, 22, 1225–1228, https://doi.org/10.1029/95GL00881, http://agupubs.onlinelibrary.wiley.com/doi/abs/10.1029/95GL00881, 1995.

Saueressig, G., Crowley, J. N., Bergamaschi, P., Brühl, C., Brenninkmeijer, C. A. M., and Fischer, H.: Carbon 13 and D kinetic isotope effects in the reactions of CH4 with O(1 D) and OH: New laboratory measurements and their implications for the isotopic composition of stratospheric methane, Journal of Geophysical Research: Atmospheres, 106, 23 127–23 138, https://doi.org/10.1029/2000JD000120, https://agupubs.onlinelibrary.wiley.com/doi/abs/10.1029/2000JD000120, 2001.

Saunois, M., Jackson, R. B., Bousquet, P., Poulter, B., and Canadell, J. G.: The growing role of methane in anthropogenic climate change, Environmental Research Letters, 11, 120 207, https://doi.org/10.1088/1748-9326/11/12/120207, http://stacks.iop.org/1748-9326/11/i=12/a=120207?key=crossref.f1e669851e5141388b857d7785cee453, 2016.

Saunois, M., Bousquet, P., Poulter, B., Peregon, A., Ciais, P., Canadell, J. G., Dlugokencky, E. J., Etiope, G., Bastviken, D., Houweling, S., Janssens-Maenhout, G., Tubiello, F. N., Castaldi, S., Jackson, R. B., Alexe, M., Arora, V. K., Beerling, D. J., Bergamaschi, P., Blake, D. R., Brailsford, G., Bruhwiler, L., Crevoisier, C., Crill, P., Covey, K., Frankenberg, C., Gedney, N., Höglund-Isaksson, L., Ishizawa, M., Ito, A., Joos, F., Kim, H.-S., Kleinen, T., Krummel, P., Lamarque, J.-F., Langenfelds, R., Locatelli, R., Machida, T., Maksyutov, S., Melton, J. R., Morino, I., Naik, V., O'Doherty, S., Parmentier, F.-J. W., Patra, P. K., Peng, C., Peng, S., Peters, G. P., Pison, I., Prinn, R., Ramonet, M., Riley, W. J., Saito, M., Santini, M., Schroeder, R., Simpson, I. J., Spahni, R., Takizawa, A., Thornton, B. F., Tian, H., Tohjima, Y., Viovy, N., Voulgarakis, A., Weiss, R., Wilton, D. J., Wiltshire, A., Worthy, D., Wunch, D., Xu, X., Yoshida, Y., Zhang, B., Zhang, Z., and Zhu, Q.: Variability and quasi-decadal changes in the methane budget over the period 2000–2012, Atmospheric Chemistry and Physics, 17, 11 135–11 161, https://doi.org/https://doi.org/10.5194/acp-17-11135-2017, https://www.atmos-chem-phys.net/17/11135/2017/, 2017.

Saunois, M., Stavert, A. R., Poulter, B., Bousquet, P., Canadell, J. G., Jackson, R. B., Raymond, P. A., Dlugokencky, E. J., Houweling, S., Patra, P. K., Ciais, P., Arora, V. K., Bastviken, D., Bergamaschi, P., Blake, D. R., Brailsford, G., Bruhwiler, L., Carlson, K. M., Carrol, M., Castaldi, S., Chandra, N., Crevoisier, C., Crill, P. M., Covey, K., Curry, C. L., Etiope, G., Frankenberg, C., Gedney, N., Hegglin, M. I., Höglund-Isakson, L., Hugelius, G., Ishizawa, M., Ito, A., Janssens-Maenhout, G., Jensen, K. M., Joos, F., Kleinen, T., Krummel, P. B., Langenfelds, R. L., Laruelle, G. G., Liu, L., Machida, T., Maksyutov, S., McDonald, K. C., McNorton, J., Miller, P. A., Melton, J. R., Morino, I., Müller, J., Murgia-Flores, F., Naik, V., Niwa, Y., Noce, S., O'Doherty, S., Parker, R. J., Peng, C., Peng, S., Peters, G. P., Prigent, C., Prinn, R., Ramonet, M., Regnier, P., Riley, W. J., Rosentreter, J. A., Segers, A., Simpson, I. J., Shi, H., Smith, S. J., Steele, P. L., Thornton, B. F., Tian, H., Tohjima, Y., Tubiello, F. N., Tsuruta, A., Viovy, N., Voulgarakis, A., Weber, T. S., van Weele, M., van der Werf, G. R., Weiss, R. F., Worthy, D., Wunch, D., Yin, Y., Yoshida, Y., Zhang, W., Zhang, Z., Zhao, Y., Zheng, B., Zhu, Q., Zhu, Q., and Zhuang, Q.: The Global Methane Budget 2000–2017, Earth System Science Data Discussions, pp. 1–138, https://doi.org/10.5194/essd-2019-128, https://www.earth-syst-sci-data-discuss.net/essd-2019-128/, 2019.

Schaefer, H., Fletcher, S. E. M., Veidt, C., Lassey, K. R., Brailsford, G. W., Bromley, T. M., Dlugokencky, E. J., Michel, S. E., Miller, J. B., Levin, I., Lowe, D. C., Martin, R. J., Vaughn, B. H., and White, J. W. C.: A 21st-century shift from fossil-fuel to biogenic methane emissions indicated by 13CH4, Science, 352, 80–84, https://doi.org/10.1126/science.aad2705, https://science-sciencemag-org.insu.bib.cnrs.fr/content/352/6281/80, 2016.

Snover, A. K. and Quay, P. D.: Hydrogen and carbon kinetic isotope effects during soil uptake of atmospheric methane, Global Biogeochemical Cycles, 14, 25–39, https://doi.org/10.1029/1999GB900089, https://agupubs.onlinelibrary.wiley.com/doi/abs/10.1029/1999GB900089, 2000.

Solomon, S.: Stratospheric ozone depletion: A review of concepts and history, Reviews of Geophysics, 37, 275–316, https://doi.org/10.1029/1999RG900008, https://agupubs.onlinelibrary.wiley.com/doi/abs/10.1029/1999RG900008, 1999.

Stohl, A.: Stratosphere-troposphere exchange: A review, and what we have learned from STACCATO, Journal of Geophysical Research, 108, 8516, https://doi.org/10.1029/2002JD002490, http://doi.wiley.com/10.1029/2002JD002490, 2003.

Tans, P. P.: A note on isotopic ratios and the global atmospheric methane budget, Global Biogeochemical Cycles, 11, 77–81, https://doi.org/10.1029/96GB03940, https://agupubs.onlinelibrary.wiley.com/doi/abs/10.1029/96GB03940, 1997.

Thompson, R. L., Chevallier, F., Crotwell, A. M., Dutton, G., Langenfelds, R. L., Prinn, R. G., Weiss, R. F., Tohjima, Y., Nakazawa, T., Krummel, P. B., Steele, L. P., Fraser, P., O'Doherty, S., Ishijima, K., and Aoki, S.: Nitrous oxide emissions 1999 to 2009 from a global atmospheric inversion, Atmospheric Chemistry and Physics, 14, 1801–1817, https://doi.org/10.5194/acp-14-1801-2014, https://www.atmos-chem-phys.net/14/1801/2014/, 2014.

Thompson, R. L., Nisbet, E. G., Pisso, I., Stohl, A., Blake, D., Dlugokencky, E. J., Helmig, D., and White, J. W. C.: Variability in Atmospheric Methane From Fossil Fuel and Microbial Sources Over the Last Three Decades, Geophysical Research Letters, 45, 11,499–11,508, https://doi.org/10.1029/2018GL078127, https://agupubs.onlinelibrary.wiley.com/doi/abs/10.1029/2018GL078127, 2018.

Tiedtke, M.: A Comprehensive Mass Flux Scheme for Cumulus Parameterization in Large-Scale Models, Monthly Weather Review, 117, 1779–1800, https://doi.org/10.1175/1520-0493(1989)117<1779:ACMFSF>2.0.CO;2, https://journals.ametsoc.org/doi/abs/10.1175/1520-0493%281989%29117%3C1779%3AACMFSF%3E2.0.CO%3B2, 1989.

Turner, A. J., Frankenberg, C., and Kort, E. A.: Interpreting contemporary trends in atmospheric methane, Proceedings of the National Academy of Sciences, 116, 2805–2813, https://doi.org/10.1073/pnas.1814297116, https://www.pnas.org/content/116/8/2805, 2019.

Tyler, S. C., Crill, P. M., and Brailsford, G. W.: 13C12C Fractionation of methane during oxidation in a temperate forested soil, Geochimica et Cosmochimica Acta, 58, 1625–1633, https://doi.org/10.1016/0016-7037(94)90564-9, http://www.sciencedirect.com/science/article/pii/0016703794905649, 1994.

van der Werf, G. R., Randerson, J. T., Giglio, L., van Leeuwen, T. T., Chen, Y., Rogers, B. M., Mu, M., van Marle, M. J. E., Morton, D. C., Collatz, G. J., Yokelson, R. J., and Kasibhatla, P. S.: Global fire emissions estimates during 1997–2016, Earth System Science Data, 9, 697–720, https://doi.org/10.5194/essd-9-697-2017, https://www.earth-syst-sci-data.net/9/697/2017/, 2017.

Von Clarmann, T.: Chlorine in the stratosphere, Atmósfera, 26, 415–458, https://doi.org/10.1016/S0187-6236(13)71086-5, http://www.revistascca.unam.mx/atm/index.php/atm/article/view/38656/36823, 2013.

Wang, J. S., McElroy, M. B., Spivakovsky, C. M., and Jones, D. B. A.: On the contribution of anthropogenic Cl to the increase in ^{13}C of atmospheric methane: ANTHROPOGENIC Cl AND ^{13}C OF METHANE, Global Biogeochemical Cycles, 16, 20–1–20–11, https://doi.org/10.1029/2001GB001572, http://doi.wiley.com/10.1029/2001GB001572, 2002.

Wang, X., Jacob, D. J., Eastham, S. D., Sulprizio, M. P., Zhu, L., Chen, Q., Alexander, B., Sherwen, T., Evans, M. J., Lee, B. H., Haskins, J. D., Lopez-Hilfiker, F. D., Thornton, J. A., Huey, G. L., and Liao, H.: The role of chlorine in global tropospheric chemistry, Atmospheric Chemistry and Physics, 19, 3981–4003, https://doi.org/10.5194/acp-19-3981-2019, https://www.atmos-chem-phys.net/19/3981/2019/, 2019.

Warwick, N. J., Cain, M. L., Fisher, R., France, J. L., Lowry, D., Michel, S. E., Nisbet, E. G., Vaughn, B. H., White, J. W. C., and Pyle, J. A.: Using delta13C-CH4 and deltaD-CH4 to constrain Arctic methane emissions, Atmospheric Chemistry and Physics, 16, 14 891–14 908, https://doi.org/10.5194/acp-16-14891-2016, http://www.atmos-chem-phys.net/16/14891/2016/, 2016.